

Phenomenology of Supersymmetric Gauge-Higgs Unification

F. Brümmer^a, S. Fichet^b, A. Hebecker^c, S. Kraml^b

^a *Institute for Particle Physics Phenomenology, Durham University,
Durham DH1 3LE, UK*

^b *Laboratoire de Physique Subatomique et de Cosmologie, UJF Grenoble 1,
CNRS/IN2P3, 53 Avenue des Martyrs, F-38026 Grenoble, France*

^c *Institut für Theoretische Physik, Universität Heidelberg, Philosophenweg 16 und 19,
D-69120 Heidelberg, Germany*

Abstract

Supersymmetric Gauge-Higgs Unification is a well-motivated new physics scenario, both in heterotic model building and from the perspective of higher-dimensional Grand Unified Theories. When combined with radion mediated supersymmetry breaking, it allows for very specific predictions concerning the high-scale parameters of the MSSM. Using an appropriately modified version of a standard RGE evolution code (SuSpect), we derive low-scale predictions which can be tested at the LHC. The phenomenological success of our setting depends crucially on the 5d Chern–Simons term, which has not been used in previous, less encouraging studies of gauge–Higgs unification in supersymmetry.

1 Introduction

If the LHC discovers supersymmetry, it will be a great challenge to relate the measured electroweak-scale parameters of the supersymmetric Standard Model to more fundamental structures at a high energy scale. One of the best-motivated physics proposals in this context is supersymmetric grand unification [1, 2]. However, SUSY grand unification by itself places only rather limited constraints on the low-energy parameter space.

An elegant and natural further idea making this setting more predictive is gauge–Higgs unification (GHU). In models of this type, some or all of the Higgs scalars are extra-dimensional components of gauge fields.¹ GHU is for instance realized in many grand-unified models derived from heterotic string theory, where one or both of the MSSM Higgs doublets can come from the untwisted sector (see e.g. [4]; for a recent review see [5]). At a simpler level, GHU can be realized in purely field-theoretic 5d or 6d orbifold GUT models [6]. These can be viewed as effective unified field theories, valid directly below the heterotic string scale. Such constructions receive independent support from the string-scale/GUT-scale problem [7] as follows: One of the possibilities for overcoming this problem is the compactification on anisotropic orbifolds [8–11], where one or two of the compactification radii are much larger than the string length scale. This naturally allows for an intermediate effective description in terms of a 5d or 6d orbifold GUT.

The present paper, which is mainly phenomenologically oriented, does not depend on specific string-theoretic realizations of GHU. Our analysis relies only on simple SUSY field theory models in which GHU can arise, and whose 4d low-energy effective field theory is the MSSM. The earliest and simplest construction of this type is the 5d SU(6) model of Burdman and Nomura [12], which we will largely follow. We expect, however, that our phenomenological results will carry over to similar models, including more elaborate string-derived constructions. Related models include, e.g., the 5d SU(6) model with warped extra dimensions of [13] and the 6d models of [14–16]. For more work on SUSY GHU in orbifold GUTs, see for instance [17] and references therein.

The main point of 5d GHU models relevant to our work is easily explained: 5d gauge symmetry enforces a Kähler potential in the Higgs sector of the form [18] (see also [19–21])

$$S \supset \int d^4x \int d^4\theta \varphi \bar{\varphi} Y_H(T, \bar{T}) (\bar{H}_1 + H_2)(\bar{H}_2 + H_1). \quad (1)$$

Here H_1 and H_2 are the MSSM Higgs superfields, arising from the adjoint of the 5d gauge group after its breaking to the Standard Model group. The prefactor Y_H is a real function of the radion superfield T , and φ is the chiral compensator of 4d supergravity. If T and φ develop F -term VEVs [22], Eq. (1) clearly induces a supersymmetric μ term as well as soft Higgs mass terms. They satisfy the relation

$$m_1^2 = m_2^2 = |m_3^2| \quad (2)$$

at the GUT scale, where $m_{1,2}^2 = |\mu|^2 + m_{H_{1,2}}^2$ are the diagonal entries of the Higgs mass matrix and $m_3^2 = B\mu$ is the off-diagonal element. This is a specific realization of the Giudice-Masiero mechanism [23] or of its string-theoretic version [24].

¹In fact, GHU has a long history in non-supersymmetric models without grand unification (see e.g. [3] and many subsequent papers). Here, we take the SUSY GUT idea as our main paradigm.

At the TeV scale, the familiar conditions for electroweak symmetry breaking and vacuum stability read:

$$\begin{aligned} m_1^2 m_2^2 - m_3^4 &< 0, \\ m_1^2 + m_2^2 - 2m_3^2 &> 0. \end{aligned} \tag{3}$$

Renormalization group (RG) running must thus turn the equalities of (2) at the UV scale into the inequalities of (3) at the weak scale. A numerical analysis is required in order to find out whether this is possible at all and, if so, whether it is possible within a realistic model. This analysis has to take into account some additional predictions of 5d GHU models. In particular, there are strict relations between the Higgs mass parameters, the gaugino mass, and the dominant soft sfermion masses and trilinear couplings.

If the function Y_H comes entirely from the gauge-kinetic term of the 5d super Yang–Mills action, one finds $Y_H \sim 1/(T + \bar{T})$. In this case, the relations between the soft parameters turn out to be rather restrictive and a realistic low-energy spectrum cannot be obtained without extreme fine-tuning [18].

If we also include a supersymmetric 5d Chern–Simons term and allow for a VEV of the chiral adjoint in the 5d gauge multiplet, an extra contribution $\sim 1/(T + \bar{T})^2$ to the function $Y_H(T, \bar{T})$ arises [25]. The Chern–Simons term is generically present in a 5d super Yang–Mills theory compactified on S^1/\mathbb{Z}_2 , and its coefficient is determined by anomaly cancellation [26, 27]. It depends on the full field content of the model, which we do not fix completely. In particular, the fields of the two light generations can be distributed in various ways between bulk and branes. The prefactor of the $1/(T + \bar{T})^2$ -contribution to Y_H depends on the coefficient of the Chern–Simons term and on the size of the adjoint VEV, which is also unknown. Hence we treat this prefactor as an extra parameter.

The main point of the present paper is to demonstrate that, allowing for this Chern–Simons term contribution to Eq. (1), a completely realistic low-energy phenomenology can be obtained. This scenario is rather constrained since all MSSM soft parameters are given in terms of the VEVs of F^T and F^φ , a dimensionless parameter c' characterizing the effect of the Chern–Simons term, and two mixing angles related to the 5d-origin of the third-generation quarks and leptons. We analyze the low-energy phenomenology of this setting and discuss observational consequences for the LHC.

To this end, we numerically solve the renormalization group evolution of the MSSM parameters, with GUT-scale boundary conditions as determined by our GHU model. This procedure has been implemented within the public MSSM spectrum generator code `Suspect 2.41` [28]. We perform two extensive parameter scans. The first one uses a rather crude estimate for boundary conditions in the sfermion sector. This is essentially a generalization of the analysis of [18], now including the effects of a Chern–Simons term and using a state-of-the-art RG code. The second scan uses realistic boundary conditions, derived from the Burdman–Nomura model [12]. It is somewhat more involved because of the specific relations between 4d Yukawa couplings and fundamental model parameters.

In both cases we find regions of parameter space where all present experimental bounds are satisfied. In particular, we can have sufficiently high Higgs and sparticle masses to evade direct search bounds, comply with B -physics constraints on rare decays, and also obtain a neutralino as the lightest supersymmetric particle (LSP) with a dark matter relic density compatible with WMAP results. We conclude that SUSY gauge–Higgs unification with

radion mediated SUSY breaking is indeed a phenomenologically viable scenario. We also point out some characteristic LHC signatures which seem to be typical for this framework.

The paper is organized as follows: In Section 2, we explain the appearance of the GHU relation, Eq. (2), in a large class of models. In Section 3, we present a concrete 5d model and give the formulas for the GUT-scale gauge- and Higgs-sector soft terms as functions of the model parameters. Section 4 contains a discussion of the expected RG running behaviour, particularly of m_3^2 , and of its consequences for identifying phenomenologically promising parameter space regions. We discuss our general setup for numerically analyzing the RGEs in Section 5. Assuming a simplified set of sfermion soft terms, we present a first such analysis in Section 6. We proceed in Section 7 by explaining how a fully realistic sfermion sector can be included in the analysis. The corresponding numerical results are presented in Section 8 and Conclusions are given in Section 9.

2 The origin of the GHU relation for Higgs mass parameters

In string-derived or orbifold GUT models, the MSSM Lagrangian will generically depend on several moduli fields. We focus on models where SUSY breaking is communicated to the MSSM predominantly through the moduli. Furthermore, we assume that the Kähler potential depends on the Higgs superfields H_1 and H_2 only in the combination $\overline{H}_1 + H_2$ and $H_1 + \overline{H}_2$. This assumption will be justified momentarily for a certain class of models. The leading part of the Higgs action then reads

$$S \supset \int d^4x \int d^4\theta \overline{\varphi} \varphi Y_H(Z^I, \overline{Z}^{\overline{J}}) (\overline{H}_1 + H_2)(\overline{H}_2 + H_1), \quad (4)$$

where Y_H is some real analytic function of the moduli fields Z^I .

In GHU models there is no superpotential contribution to the μ term. The Higgs mass parameters are therefore entirely determined by Eq. (4): For canonically normalized Higgs fields they are given by

$$\begin{aligned} m_{H_1}^2 &= m_{H_2}^2 = -F^I \overline{F}^{\overline{J}} \partial_I \partial_{\overline{J}} \log Y_H, \\ \pm\mu &= \overline{F}^{\overline{\varphi}} + \overline{F}^{\overline{I}} \partial_{\overline{I}} \log Y_H, \\ \pm B\mu &= |F^\varphi + F^I \partial_I \log Y_H|^2 - F^I \overline{F}^{\overline{J}} \partial_I \partial_{\overline{J}} \log Y_H. \end{aligned} \quad (5)$$

These equations obviously imply Eq. (2).²

If we start from a 5d model, it is straightforward to see why the Kähler potential always depends only on the combination $H_1 + \overline{H}_2$ (and its complex conjugate): Recall that

² Note the sign ambiguity in μ and $B\mu$: Simultaneously changing the signs of both μ and $B\mu$ corresponds to a redefinition of one of the Higgs fields, say H_1 , by $H_1 \rightarrow -H_1$. The signs of the Yukawa couplings can be kept unchanged by an analogous redefinition of the right-handed matter fields it couples to. The overall sign of μ and $B\mu$ cancels in the RGEs. Therefore, given a certain high-scale model, a simultaneous sign change in the last two lines of Eq. (5) will leave the absolute values of all weak-scale parameters unchanged, flipping only the signs of μ and $B\mu$ at the weak scale. The convention that $B\mu$ is positive at the weak scale then determines the signs in Eq. (5).

a generic 5d super–Yang–Mills theory contains, in terms of 4d superfields [29–31], a vector superfield and a chiral adjoint Φ . The fifth component of the gauge field, A_5 , forms the imaginary part of the scalar component of Φ . In the 5d kinetic action, the chiral adjoint appears only in the combination $\Phi + \Phi^\dagger$ [31]. The reason is that, in this combination, A_5 drops out of the lowest component of the real superfield $\Phi + \Phi^\dagger$, ensuring the absence of non-derivative couplings of A_5 .³

The decomposition of the adjoint of the 5d gauge group G in irreducible Standard Model representations is vector-like and can contain pairs of weak doublets:

$$\mathbf{Ad}(G) \rightarrow (\mathbf{1}, \mathbf{2})_{-1/2} + (\mathbf{1}, \mathbf{2})_{1/2} + \dots \quad (6)$$

If this is the case, and if the zero-modes of these doublets in Φ survive compactification and GUT symmetry breaking, they can be identified with the Higgs fields H_1 and H_2 . It is then only the combination $H_1 + \overline{H}_2$ which appears in the 4d Kähler potential.

Intriguingly, this peculiar combination of chiral superfields has also been found in heterotic $E_8 \times E_8$ orbifold models, where no use of an intermediate 5d effective theory is made [19–21]. We briefly describe the situation following [20]: The Kähler potential can be expanded as

$$K = \mathcal{K} + \mathcal{Y}_{\alpha\bar{\alpha}} A^\alpha \bar{A}^{\bar{\alpha}} + \tilde{\mathcal{Y}}_{\beta\bar{\beta}} B^\beta \bar{B}^{\bar{\beta}} + (\mathcal{Z}_{\alpha\beta} A^\alpha B^\beta + \text{h.c.}) + \dots \quad (7)$$

Here \mathcal{K} , \mathcal{Y} , $\tilde{\mathcal{Y}}$, \mathcal{Z} are functions of the moduli, and A^α and B^β are matter fields transforming in the $\mathbf{27}$ and $\overline{\mathbf{27}}$ of E_6 , respectively. Suppose that the MSSM Higgs fields H_1 and H_2 are contained in two such fields A and B . For the desired combination $H_1 + \overline{H}_2$ to appear, one needs

$$\mathcal{Y}_{A\bar{A}} = \tilde{\mathcal{Y}}_{B\bar{B}} = \mathcal{Z}_{AB} = \overline{\mathcal{Z}}_{\bar{A}\bar{B}}. \quad (8)$$

Indeed, for untwisted matter fields A, B associated with a common complex plane, it was found that

$$\mathcal{Y}_{A\bar{A}} = \tilde{\mathcal{Y}}_{B\bar{B}} = \mathcal{Z}_{AB} = \overline{\mathcal{Z}}_{\bar{A}\bar{B}} = \frac{1}{(T + \overline{T})(U + \overline{U})}, \quad (9)$$

where U and T are the complex structure and Kähler modulus of that plane. By contrast, for twisted matter fields, or for untwisted matter fields associated with distinct planes, or with a plane without U modulus, one has $\mathcal{Z}_{AB} = 0$.

We now argue that the above string-theoretic results are closely related to the previous 5d argument. Firstly, if A and B are associated with the same complex plane, one can take a 6d limit in which the two corresponding compactification radii remain large. In this limit, the fields A and B are the extra-dimensional components of the 6d gauge field. Secondly, the presence of a shape modulus U of the corresponding large T^2 allow for 5d limit, in which the compact space becomes an interval. Thus, the string-theoretic conditions which ensure that the combination $H_1 + \overline{H}_2$ appears are precisely those which are needed for an appropriate 5d limit to exist. Even in regions of moduli space which do not correspond to that limit, the structure enforced by 5d gauge invariance survives. In other words, the simple 5d argument given earlier appears to be sufficient to understand the situation in

³In fact, an analogous argument forces the Kähler potential to depend on the radion modulus T only through the combination $T + \overline{T}$. In this case, the imaginary part is the 5th component of the graviphoton of 5d supergravity, and the real combination $T + \overline{T}$ ensures the absence of non-derivative couplings of this gauge-field component [29].

heterotic orbifold models as well. It would be interesting to work this out in more detail, which is however beyond the scope of the present, mainly phenomenologically oriented paper.

As we have already emphasized in the Introduction, and as will become clear in subsequent sections, the 5d supersymmetric Chern–Simons term plays a central role in our analysis. Such a term cannot arise in the tree-level dimensional reduction of a theory with more than five dimensions. However, it is generically induced at one loop [32]. More specifically, the radiative generation of a Chern–Simons term in compactifications from 6d to 5d was discussed in [33]. Thus, the 5d Chern–Simons term is consistent with a 10d origin of the theory.

3 A concrete 5d realization

We now turn to the phenomenological prospects of concrete 5d models. Our main example will be a generalization of the SU(6) model of Burdman and Nomura [12], with a larger gauge group containing at least $U(6) = SU(6) \times U(1)$. The 5d gauge theory is compactified on $S^1/(\mathbb{Z}_2 \times \mathbb{Z}_2)$. The only relevant modulus is the radion superfield $T = \rho + iB_5 + \dots$, where B_5 is the fifth component of the graviphoton. The real part ρ is normalized such that $2\pi\rho$ is the volume of the original S^1 . We assume that it is eventually stabilized at $\langle \rho \rangle = R$. The Higgs doublets are contained in the superfield $\Phi = \Sigma + iA_5 + \dots$ (where Σ is the chiral adjoint of the 5d gauge multiplet, and A_5 is the fifth component of the gauge boson).

The U(1) gauge factor is assumed to be broken on the boundary. Furthermore, orbifold boundary conditions for the gauge fields can be chosen such [12] that the remaining SU(6) is broken in 4d to the Standard Model,⁴ and that the only components of Φ with zero modes are the Higgs fields. Their origin is particularly obvious in the SU(5)-decomposition

$$\mathbf{35} = \mathbf{24} + \mathbf{5} + \bar{\mathbf{5}} + \mathbf{1} \quad (10)$$

of the adjoint of SU(6). Our fields H_1 and H_2 are the doublets contained in the $\bar{\mathbf{5}}$ and $\mathbf{5}$ respectively.

Before orbifolding, the 4d effective theory contains the full gauge multiplet and chiral adjoint Φ as well as the radion T . The corresponding leading-order action, which has been analyzed in [29], contains a term

$$S \supset \frac{\pi R}{g_5^2} \int d^4x \int d^4\theta \bar{\varphi} \varphi \frac{2R}{T + \bar{T}} \text{tr} (\Phi + \Phi^\dagger)^2. \quad (11)$$

Retaining only the Φ components that survive the orbifold projection, i.e. the Higgs fields, this becomes [18]

$$S \supset \frac{2\pi R}{g_5^2} \int d^4x \int d^4\theta \bar{\varphi} \varphi \frac{2R}{T + \bar{T}} (\bar{H}_1 + H_2)(\bar{H}_2 + H_1). \quad (12)$$

Note that the coupling of T to the Higgs fields depends on the choice of Kähler–Weyl frame. We work in a frame where $K = -3 \log(T + \bar{T} + \dots)$. The 4d metric has not been rescaled after compactification.

⁴ Apart from an extra U(1) which is Higgsed by a brane field.

The 5d theory will in general also contain a Chern–Simons term. Its supersymmetrized version includes a cubic term in Φ , which couples to the radion according to [25]

$$S \supset \frac{c\pi R}{3} \int d^4x \int d^4\theta \bar{\varphi}\varphi \left(\frac{2R}{T+\bar{T}} \right)^2 \text{tr} (\Phi + \bar{\Phi})^3. \quad (13)$$

After orbifolding and allowing for a non-zero expectation value $\langle \Phi \rangle = v \mathbb{1}_6$, this part of the Chern–Simons action contributes as

$$S \supset \frac{2c'\pi R}{g_5^2} \int d^4x \int d^4\theta \bar{\varphi}\varphi \left(\frac{2R}{T+\bar{T}} \right)^2 (\bar{H}_1 + H_2)(\bar{H}_2 + H_1) \quad (14)$$

to the quadratic Higgs Lagrangian.⁵ Here we have introduced the dimensionless constant $c' = 2cvg_5^2$. Note that the group $U(6) = SU(6) \times U(1)$, which we use here and below, is only the simplest extension of $SU(6)$ allowing for an $SU(6)$ -preserving Φ -VEV.⁶ Larger and, in particular, simple groups, such as $SU(7)$, are clearly possible.

We regard c' as a free parameter for the purpose of our analysis: While boundary-anomaly cancellation fixes c for a given field content, we specify neither this field content nor the value of v . In particular, different distributions of the light generations between the two branes affect the value of c . However, positivity of the kinetic terms (given just below) leads to the constraint

$$c' > -1. \quad (15)$$

The MSSM scalar potential for canonically normalized Higgs fields (which we also call H_1 and H_2 by abuse of notation) reads, at quadratic order,

$$V = m_1^2 |H_1|^2 + m_2^2 |H_2|^2 + m_3^2 (H_2 H_1 + \text{h.c.}). \quad (16)$$

The mass parameters m_i^2 can now be calculated from the Higgs kinetic function

$$Y_H(T, \bar{T}) = \frac{\pi R}{g_5^2} \left(1 + c' \frac{2R}{T+\bar{T}} \right) \frac{2R}{T+\bar{T}}, \quad (17)$$

which follows from Eqs. (12) and (14). According to Eqs. (5), the parameters μ and m_i^2 read [25]

$$\epsilon_H \mu = \bar{F}^{\bar{\varphi}} - \frac{\bar{F}^T}{2R} \frac{1+2c'}{1+c'}, \quad (18)$$

$$m_1^2 = m_2^2 = \epsilon_H m_3^2 = |F^\varphi|^2 - \frac{(F^\varphi \bar{F}^T + \text{h.c.})}{2R} \frac{1+2c'}{1+c'} + \frac{|F^T|^2}{(2R)^2} \frac{2c'^2}{(1+c')^2}, \quad (19)$$

where we have introduced a parameter $\epsilon_H = \pm 1$ to account for the sign ambiguity in $m_3^2 = B\mu$ and μ .

From the 5d gauge-kinetic and Chern–Simons action we obtain, after dimensional reduction,

$$S \supset \frac{\pi R}{g_5^2} \int d^4x \int d^2\theta \frac{T}{R} \text{tr} W^\alpha W_\alpha + \text{h.c.} + 2c\pi R \int d^4x \int d^2\theta \text{tr} (\Phi W^\alpha W_\alpha) + \text{h.c.}, \quad (20)$$

⁵Our Φ -VEV $v = v_{4d}$ is a VEV in the 4d effective theory. It is related to the corresponding VEV v_{5d} of the underlying 5d theory by $v_{4d} = (\rho/R)v_{5d}$. Here the mass dimensions of the 4d and 5d scalar fields are the same since we assume that the complete leading-order 5d Lagrangian has a prefactor $1/g_5^2$.

⁶The significantly more complicated case of $SU(6)$ -breaking expectation values is considered in [25].

which eventually gives the 4d gauge-kinetic term

$$S \supset \frac{\pi R}{g_5^2} \int d^4x \int d^2\theta \left(\frac{T}{R} + c' \right) \text{tr} W^\alpha W_\alpha + \text{h.c.} . \quad (21)$$

It determines the gaugino masses ⁷

$$M_{1/2} = \frac{\overline{F}^T}{2R} \frac{1}{1 + c'} \quad (22)$$

as well as the 4d gauge coupling

$$\frac{1}{g_4^2} = \frac{2\pi R}{g_5^2} (1 + c') . \quad (23)$$

The soft masses and trilinear terms for the matter multiplets are more model-dependent. Quite generally the relevant piece of the kinetic action can be written as

$$S \supset \int d^4x \int d^4\theta \overline{\varphi} \varphi \left[Y_U(T, \overline{T}) |U|^2 + Y_Q(T, \overline{T}) |Q|^2 + Y_D(T, \overline{T}) |D|^2 \right. \\ \left. + Y_E(T, \overline{T}) |E|^2 + Y_L(T, \overline{T}) |L|^2 + Y_N(T, \overline{T}) |N|^2 \right] . \quad (24)$$

The kinetic functions Y_X (with $X = U, D, Q, E, N, L$ standing for up-type and down-type right-handed quarks, quark doublets, charged and uncharged right-handed leptons and lepton doublets) determine the soft masses according to

$$m_X^2 = -|F^T|^2 \frac{\partial^2}{\partial T \partial \overline{T}} \log Y_X(T, \overline{T}) . \quad (25)$$

The trilinear couplings are given by

$$A_{U,D} = F^T \frac{\partial}{\partial T} \log (Y_H Y_Q Y_{U,D}) , \quad (26)$$

$$A_E = F^T \frac{\partial}{\partial T} \log (Y_H Y_L Y_E) . \quad (27)$$

Note that we define the A term with a negative sign in the Lagrangian:

$$\mathcal{L} \supset - \left(A_U y_U H_2 \tilde{Q} \tilde{U} + A_D y_D H_1 \tilde{Q} \tilde{D} + A_E y_E H_1 \tilde{L} \tilde{E} + \text{h.c.} \right) . \quad (28)$$

The precise form of the matter kinetic functions depends on the model under consideration. We will assume throughout that the first two generations of MSSM matter are brane-localized and that their GUT-scale soft terms are negligible. This gives no-scale boundary conditions for the first and second generation. For the third generation, we will consider two cases: first the approximation that only the top quark receives a Yukawa coupling induced by the 5d gauge coupling, and second the case of the Burdman–Nomura model with realistic top, bottom and tau Yukawa couplings.

⁷ Note that this agrees with [25] only after a substitution $c' \rightarrow c'/2$, which is due to our modified definition of c' . However, after this substitution, it becomes apparent that Eqs. (18) and (19) are truly different from [25]. This is the result of our SU(6)-preserving Φ -VEV, as opposed to the SU(6)-breaking Φ -VEV of [25].

4 Expected running patterns

Before we present the numerical results, let us briefly discuss what general features we expect. Needless to say, the complete system of two-loop renormalization group equations (RGEs), which will be solved numerically in the following sections, is far too complicated to permit an analytical treatment. Some aspects can nevertheless be qualitatively understood by inspection of the dominant contributions to the one-loop RGEs.

The scale of electroweak symmetry breaking (EWSB) is defined as usual as the geometric mean of the stop masses, $M_{\text{EWSB}} = \sqrt{m_{\tilde{t}_1} m_{\tilde{t}_2}}$. At this scale the conditions of Eq. (3) have to hold. Once EWSB occurs, one finds the well-known relations between μ , $B\mu = m_2^2$, M_Z , the Higgs soft masses $m_{H_i}^2$ and the ratio $\tan\beta$ of Higgs expectation values:

$$\begin{aligned}\mu^2 &= \frac{1}{2} [\tan 2\beta (m_{H_2}^2 \tan\beta - m_{H_1}^2 \cot\beta) - M_Z^2], \\ B\mu &= \frac{1}{2} \sin 2\beta [m_{H_1}^2 + m_{H_2}^2 + 2\mu^2].\end{aligned}\tag{29}$$

We focus on the region of moderately large $\tan\beta$, roughly $\tan\beta \gtrsim 5$, to ensure that the tree-level bound on the lightest Higgs mass, $m_h \leq M_Z$, is approximately saturated. The Higgs mass can then be lifted above the direct search limit by radiative corrections, mainly due to stop loops.

The latter involves a significant fine-tuning (the notorious MSSM ‘‘little hierarchy problem’’), because the soft mass scale must be large compared to M_Z instead of being of the same order of magnitude, which would be the natural situation. For sizeable $\tan\beta$ one has

$$\frac{M_Z^2}{2} \approx -m_2^2,\tag{30}$$

so m_2^2 must be negative and small compared to typical soft masses. We will not discuss this fine-tuning any further (see however [34]), but accept it and focus on the implications for models with GHU boundary conditions. One immediate consequence is that $m_2^2 > 0$ at the GUT scale, because the soft mass $m_{H_2}^2$ and hence also m_2^2 runs down towards lower energies (the running of μ is insignificant). While this also fixes the GUT-scale sign of m_1^2 to be positive, either sign for $B\mu$ is possible (cf. Eq. 5). In other words, we can have $\epsilon_H = +1$ or $\epsilon_H = -1$ in the GHU relations

$$m_{H_1}^2 = m_{H_2}^2 = \epsilon_H B\mu - |\mu|^2.\tag{31}$$

However, as we will now argue, ϵ_H is always determined by the sign of μ : Out of the four sign choices $\mu > 0$ or $\mu < 0$ and $\epsilon_H = \pm 1$, only two can generically lead to realistic spectra. To establish this observe first that m_1^2 will typically not evolve by more than a factor of 2 – 3, and therefore remains of the order of magnitude of the typical soft mass scale during RG running. Furthermore, we just stated that m_2^2 at M_{EWSB} should be small compared to the typical soft mass scale, and that $\tan\beta$ should at least be moderately large. From all this it follows that $B\mu$ at the EWSB scale should be small compared to the typical soft mass-squared scale as well, as can be read off from

$$\tan\beta + \cot\beta = \frac{m_1^2 + m_2^2}{2B\mu}\tag{32}$$

(which is equivalent to the second line of Eqs. (29)). We will now show that requiring small EWSB-scale $B\mu$ generically fixes ϵ_H in terms of $\text{sign}(\mu)$.

The RG evolution of $B\mu$ is primarily governed by the terms involving the top trilinear coupling and the weak gaugino mass:

$$16\pi^2 \frac{d}{dt} B\mu = \mu(6A_t|y_t|^2 + 6g_2^2 M_2) + \dots \quad (33)$$

We can choose positive gaugino masses without loss of generality. Let us now discuss the relevance of the two dominant terms on the r.h. side of Eq. (33):

The gluino contribution to the A_t -RGE forces A_t to run negative towards low scales. This is fairly universal, i.e. more or less independent of the values of the other parameters. The value of A_t at any given scale is thus to a good approximation dictated only by its GUT-scale boundary value and $M_{1/2}$. The running of gaugino masses is also approximately universal: at one-loop, they simply evolve according to the respective gauge coupling beta functions. In the RG evolution of $B\mu$, A_t will therefore always dominate at low energies, when it has become large and negative and when also y_t has grown large. Correspondingly, the M_2 term on the r.h. side of Eq. (33) can dominate only at energies near M_{GUT} , before it is overwhelmed by A_t .

For negative μ , $B\mu$ initially increases from its GUT-scale value and then runs down; for positive μ , it evolves in the opposite way. The relative importance of the A_t and the M_2 contributions is set by their GUT-scale initial values: the larger A_t at M_{GUT} , the longer it will take to run negative and to finally dominate the $B\mu$ RG evolution. For small or negative GUT-scale A_t , the $B\mu$ running at low energies is more important than the initial, M_2 -dominated phase near M_{GUT} .

The direction and slope of the running of $B\mu$ are set by the sign and magnitude of μ , which itself does not run significantly as mentioned. We observed before that $B\mu$ should be small at the EWSB scale — for the sake of the argument, let us try to construct a situation where it is exactly zero. It should in particular change significantly with respect to its initial GUT-scale value, so $|\mu|$ should be sizeable. Furthermore, changing the sign of μ will lead to $B\mu$ evolving in the opposite way (at least as far as the evolution is governed by the terms in Eq. (33)). If there is a solution with, e.g., $\epsilon_H = -1$ and $\text{sign}(\mu) = -1$, we therefore expect a nearby mirror solution for the opposite sign choice. On the other hand, changing only one of the signs will generically not lead to a solution due to the approximately universal behaviour of A_t and M_2 . We have sketched this behaviour in Fig. 1 for large GUT-scale A_t , and in Fig. 2 for small or negative GUT-scale A_t .

Thus, while one might naively have expected four branches of solutions of the RGEs to give realistic spectra (corresponding to the two choices of each $\text{sign}(\mu)$ and of ϵ_H), by the above discussion there should in fact appear only two. Furthermore, we expect sizeable $|\mu|$ in all cases.

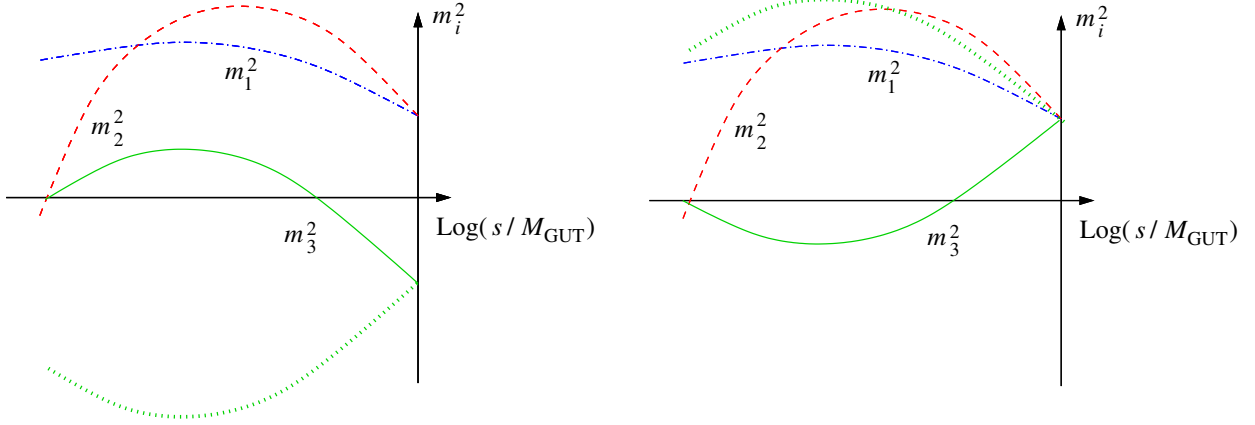


Figure 1: Qualitative RG evolution of m_1^2 (blue dot-dashed curve), m_2^2 (red dashed curve), and m_3^2 (green solid curve) as a function of the scale s , between $s = M_{\text{EWSB}}$ and $s = M_{\text{GUT}}$. A_t at the GUT scale is sizeable and positive. The green dotted curve is m_3^2 for the wrong $\text{sign}(\mu)$, which does not lead to realistic EWSB. Left panel: $\epsilon_H = -1$ requires $\text{sign}(\mu) = -1$. Right panel: $\epsilon_H = +1$ requires $\text{sign}(\mu) = +1$.

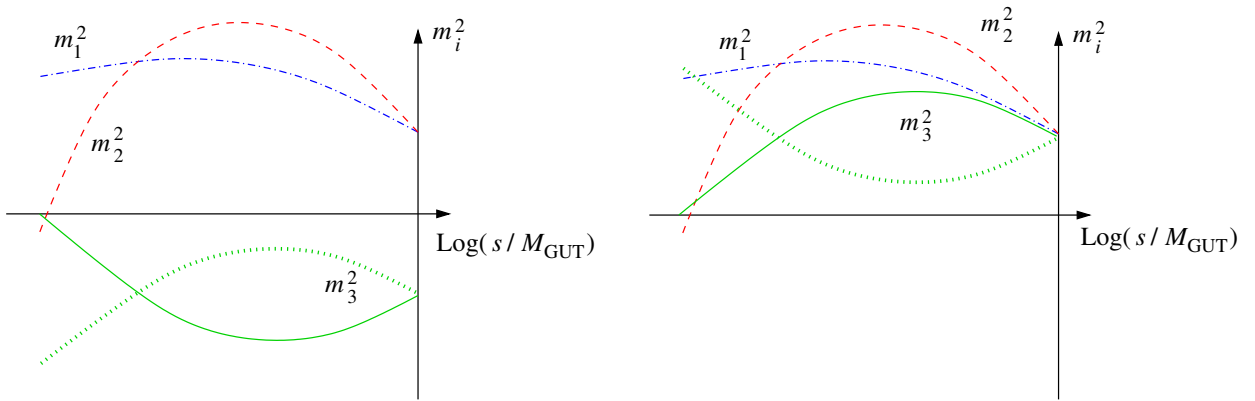


Figure 2: Same as Fig. 1 for small or negative GUT-scale A_t . Left panel: $\epsilon_H = -1$ requires $\text{sign}(\mu) = +1$. Right panel: $\epsilon_H = +1$ requires $\text{sign}(\mu) = -1$.

5 Numerical analysis: General setup

For the numerical analysis, we make use of the public state-of-the-art SUSY spectrum code `Suspect 2.41` [28], appropriately modified to be applied to our SUSY GHU model. The usual procedure in `Suspect` and in other SUSY spectrum codes is to use $\tan\beta$ and M_Z as inputs and to compute μ and $B\mu$ from the EWSB condition Eqs. (29). In our model, however, the Higgs soft masses and μ and $B\mu$ are not independent, since they are related by the GHU conditions (31) at the GUT scale.

The free parameters in the gauge–Higgs sector of the model are actually $F^T/2R$, F^φ and c' , from which the GUT-scale values for $M_{1/2}$, μ , $B\mu$ and $m_{H_{1,2}}^2$ are determined according to Eqs. (18), (19) and (22). Together with the GUT-scale values for the sfermion mass parameters and trilinear couplings, they furnish a set of GUT-scale boundary conditions for the MSSM renormalization group equations.

It is in principle possible to change the usual procedure of spectrum computation such

that μ and $B\mu$ become high-scale inputs, while $\tan\beta$ as well as M_Z are output determined by Eq. (29). We have implemented this scheme in **Suspect 2.41**; the requirement to find the correct experimental value of M_Z , however, makes parameter scans very inefficient.

For the present analysis we have therefore chosen a different approach: We work with the conventional SUGRA scheme of **Suspect 2.41**, which takes $\tan\beta(M_Z)$ together with the GUT-scale values of all soft-breaking parameters except $B\mu$ as input. We only modify this scheme by not specifying fixed GUT-scale values for the Higgs soft masses $m_{H_1}^2$ and $m_{H_2}^2$, but instead determining them from the GHU boundary conditions Eq. (31).

Our input parameters are thus $M_{1/2}(M_{\text{GUT}})$ and $\tan\beta(M_Z)$, the two sign coefficients $\text{sign}(\mu)$ and ϵ_H , plus the sfermion mass parameters and A -terms at M_{GUT} . The values of μ , $B\mu$, $m_{H_1}^2$, $m_{H_2}^2$ are computed iteratively applying Eqs. (29) at the EWSB scale and Eq. (31) and the GUT scale. When a stable solution is found, the model parameters $F^T/2R$, F^φ and c' are inferred from $M_{1/2}$, μ and $B\mu$ at M_{GUT} by inverting Eqs. (18), (19) and (22).

A complication arises, however, from the sfermion sector. As discussed in Section 3, we assume no-scale boundary conditions, i.e. a common scalar mass $m_0 \equiv 0$ and a common trilinear coupling $A_0 \equiv 0$, for squarks and sleptons of the first two generations. The soft terms of the third generation, on the other hand, can be non-zero. To be more precise, they will depend on $F^T/2R$ and c' (and possibly also on other model parameters) according to their kinetic functions. This requires an extra level of iteration in the spectrum computation.

It turns out to be convenient to let this iteration act on c' . We thus start the procedure described above with an initial guess of c' , which is kept constant until a first convergence of the spectrum is reached. This has the virtue that the GUT-scale sfermion soft masses are unambiguously fixed in terms of c' , $M_{1/2}$, and other input parameters (as will become clear once we describe how we are modelling the matter sector) so the EWSB scale does not change too much in each iteration step, which could lead to numerical instabilities. When convergence is reached, an updated value of c' as computed from $M_{1/2}$, μ and $B\mu$ is taken as the new input c' , and the whole procedure is iterated until c' converges as well.

Let us finally list the Standard Model (SM) input values and experimental constraints. For the SM input values, we take $\alpha^{-1}(M_Z) = 127.934$, $\alpha_s(M_Z) = 0.1172$ and $m_b(m_b) = 4.25$ GeV in the \overline{MS} scheme, and an onshell top mass of $m_t = 172.4$ GeV [35]. Moreover, $M_Z = 91.187$ and $m_\tau = 1.777$ GeV, and $G_F = 1.16639 \cdot 10^{-5}$ GeV⁻².

To take into account the limits from direct SUSY searches at LEP [36], we require $m_{\tilde{\chi}_1^\pm} > 103.5$ GeV and $m_{\tilde{e}, \tilde{\mu}} > 100$ GeV. The limit on $m_{\tilde{\tau}_1}$ is parametrized as a function of $m_{\tilde{\chi}_1}$ as given by [36]; in case of a stau LSP, we take $m_{\tilde{\tau}_1} > 94$ GeV. For the light scalar Higgs, we apply the limits from LEP for the m_h^{max} scenario given in [37], taking into account a ~ 2 GeV theoretical error [38].⁸

We also take into account additional constraints from B -physics. For the branching ratio of inclusive radiative B decay, we use the experimental result $\text{BR}(b \rightarrow s\gamma) = (3.52 \pm 0.23 \pm 0.09) \times 10^{-4}$ from HFAG [39], together with the SM theoretical prediction of $\text{BR}(b \rightarrow s\gamma)^{\text{SM}} = (3.15 \pm 0.23) \times 10^{-4}$ of [40]. Combining experimental and theoretical errors in quadrature, we require $2.85 \leq \text{BR}(b \rightarrow s\gamma) \times 10^4 \leq 4.19$ at 2σ . Another important

⁸Moreover, the limits from direct squark and gluino searches at the Tevatron for $m_{\tilde{q}} \simeq m_{\tilde{g}}$ apply, in particular $m_{\tilde{g}} > 392$ GeV, but these are automatically fulfilled here.

constraint comes from the B_s decay into a pair of muons. Here we apply the 95% CL upper limit $\text{BR}(B_s \rightarrow \mu^+\mu^-) < 5.8 \times 10^{-8}$ from CDF [41]. Regarding the anomalous magnetic moment of the muon, we do not impose any limits but simply note that $(g-2)_\mu$ favours $\mu > 0$.

Last but not least, if the lightest neutralino is the LSP, we compare its relic density to the results from the 5-year WMAP data on the dark matter relic density, $\Omega h^2 = 0.1099 \pm 0.0062$ [42], although we do not impose this as a strict constraint. The values of $\text{BR}(b \rightarrow s\gamma)$, $\text{BR}(B_s \rightarrow \mu^+\mu^-)$ and Ωh^2 are computed using the `micrOMEGAs2.2` package [43].

6 Results for simplified boundary conditions

Here we perform a first exploration of the parameter space using simplified boundary conditions in the matter sector according to [18]. More precisely, we assume that not only the first two generations but also the third-generation leptons and r.h. bottom are brane-localized. The top and l.h. bottom have a flat profile in the fifth dimension. The relevant kinetic functions then are⁹

$$Y_{Q_3} \approx Y_{U_3} \approx \frac{\pi}{2}(T + \bar{T}), \quad (34)$$

which leads to

$$m_{Q_3}^2 \approx m_{U_3}^2 \approx \left| \frac{F^T}{2R} \right|^2 \quad (35)$$

and

$$A_t \approx \frac{F^T}{2R} \frac{1}{1+c'}. \quad (36)$$

The setup for the first parameter scan is therefore as follows:

- We vary $M_{1/2}$ from 100 and 1000 GeV and $\tan\beta$ from 2 and 20. (For higher values of $\tan\beta$, the bottom Yukawa coupling would be no longer negligible.)
- We set $m_{U_3}^2 = m_{Q_3}^2 = M_{1/2}^2(1+c')^2$ and $A_t = M_{1/2}$; this requires the additional iteration on c' as detailed in Section 5. All other sfermion soft terms are assumed to be zero at the GUT scale.
- We allow for all four sign combinations of $\text{sign}(\mu) = \pm 1$ and $\epsilon_H = \pm 1$.
- μ and $B\mu$ are determined from Eq. (29) at the EWSB scale, while $m_{H_1}^2$ and $m_{H_2}^2$ are determined from Eq. (31) at M_{GUT} .
- For each point that gives correct EWSB, we check the mass limits from LEP as well as the constraints from $\text{BR}(b \rightarrow s\gamma)$ and $\text{BR}(B_s \rightarrow \mu^+\mu^-)$ given in Section 5

Figure 3 shows the result of this scan in the $\tan\beta$ versus $M_{1/2}$ plane. As expected, correct EWSB is obtained only for two of the four possible combinations of $\text{sign}(\mu)$ and ϵ_H . In particular, it turns out that the two signs need to be equal. This is a consequence of

⁹In this approximation $y_t = g_4$ is the only non-vanishing Yukawa coupling. We will however not enforce this in the numerical analysis.

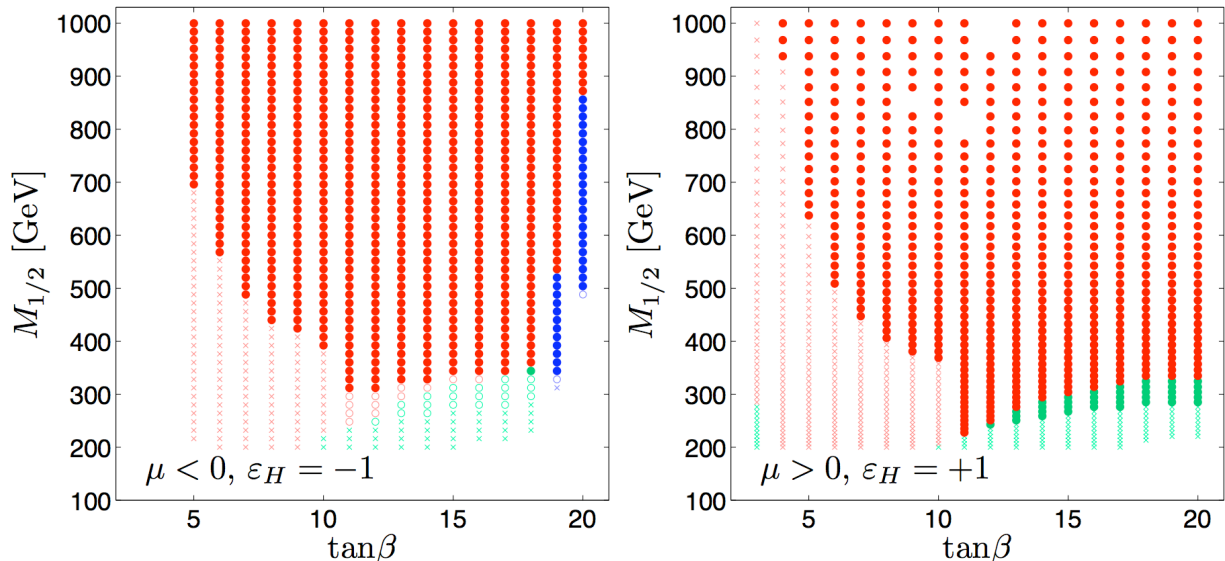


Figure 3: Parameter points giving correct EWSB from a scan over $M_{1/2}$ and $\tan\beta$ with simplified boundary conditions. The red, green and blue points have a neutralino, stau and selectron LSP, respectively. Small crosses denote points excluded by LEP, while open circles denote points excluded by B-physics constraints. The big full dots pass these constraints.

the relation $A_t = M_{1/2}$, in accord with the discussion in Section 4. Phenomenological bounds further constrain the parameter space. Points marked as small crosses in Fig. 3 are excluded by the mass bounds from LEP, while points shown as open circles are excluded by $\text{BR}(b \rightarrow s\gamma)$; the constraint from $\text{BR}(B_s \rightarrow \mu^+\mu^-)$ has no effect. The remaining big full points are phenomenologically viable. The different colours denote the nature of the LSP: red for a neutralino, blue for a selectron¹⁰, and green for a stau LSP. As one can see, most of the parameter space features a neutralino LSP, which is interesting in point of view of dark matter.¹¹ As anticipated in Section 4, $|\mu|$ turns out to be large throughout the parameter space. Numerically we find $|\mu| \sim (2.5 - 3.5)M_{1/2}$ for $\mu > 0$ and $|\mu| \sim (2.5 - 4)M_{1/2}$ for $\mu < 0$; in both cases the values at the high end are obtained for larger $\tan\beta$. The $\tilde{\chi}_1^0$ is hence almost a pure bino, and the $\tilde{\chi}_2^0$ and $\tilde{\chi}_1^\pm$ almost pure winos.

The projections onto the space of fundamental model parameters $F^T/2R$, F^φ and c' are shown in Fig. 4. We observe that for both, $\mu < 0$ and $\mu > 0$, there is a strong correlation between F^φ and $F^T/2R$, with roughly $F^\varphi \sim 3 \times F^T/2R$. This comes from setting $A_t = M_{1/2}$, which enforces $\epsilon_H = \text{sign}(\mu)$. It translates into a large value of F^φ , because $F^\varphi = \epsilon_H \mu + F^T/2R \frac{1+2c'}{1+c'}$ from Eq. (18). Nevertheless F^φ is small enough so that contributions from anomaly mediation, being $\mathcal{O}(F^\varphi/8\pi^2)$, can safely be neglected.

It is particularly interesting to note that we find no valid spectra for which $c' = 0$. This also holds when considering points excluded by LEP constraints. In this sense our analysis

¹⁰Selectrons and smuons are taken to be mass-degenerate. Here and in the following we only refer to selectrons for simplicity, implicitly meaning “selectrons and smuons”.

¹¹Alternative dark matter candidates would be gravitino or axino. A rough estimate for a no-scale radion Kähler potential $K = -3 \log(T + \bar{T})$ gives $m_{3/2} > |F^T/2R|$, while $m_{\tilde{\chi}_1^0} \simeq 0.4 M_{1/2}$. In this case a gravitino LSP is only possible for $c' < -0.6$, which does not occur in our analysis. Moreover, we expect other contributions from hidden sectors to further increase $m_{3/2}$. An axino LSP is a valid option, but leads to a very different phenomenology, beyond the scope of this paper.

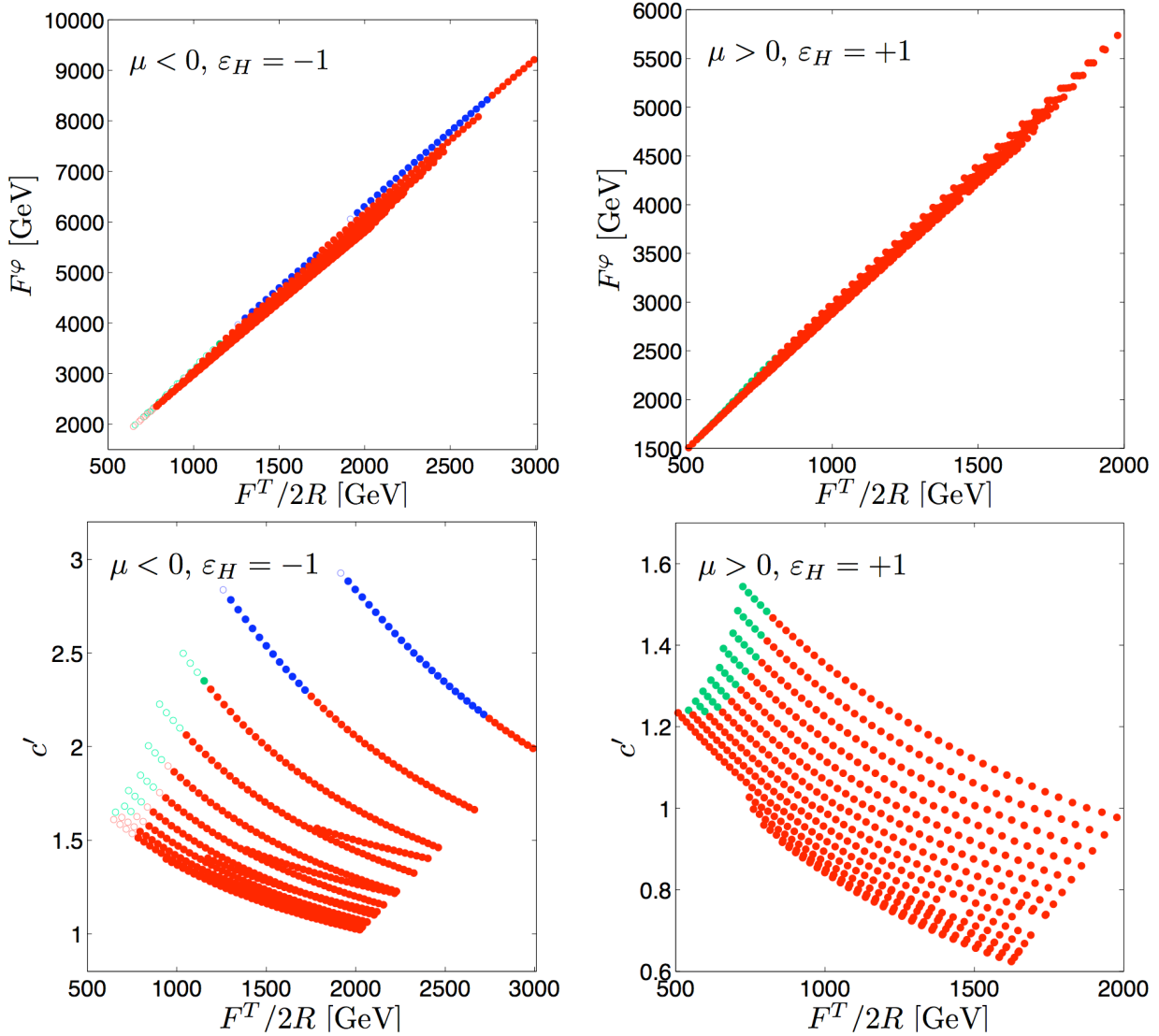


Figure 4: Scatter plot of points which give a valid spectrum solution in the $F^T/2R$ vs. F^φ plane (top row) and in the $F^T/2R$ vs. c' plane (bottom row). The red, green and blue points have a neutralino, stau and selectron LSP, respectively. Open circles denote points excluded by B-physics constraints. Points excluded by LEP are not shown.

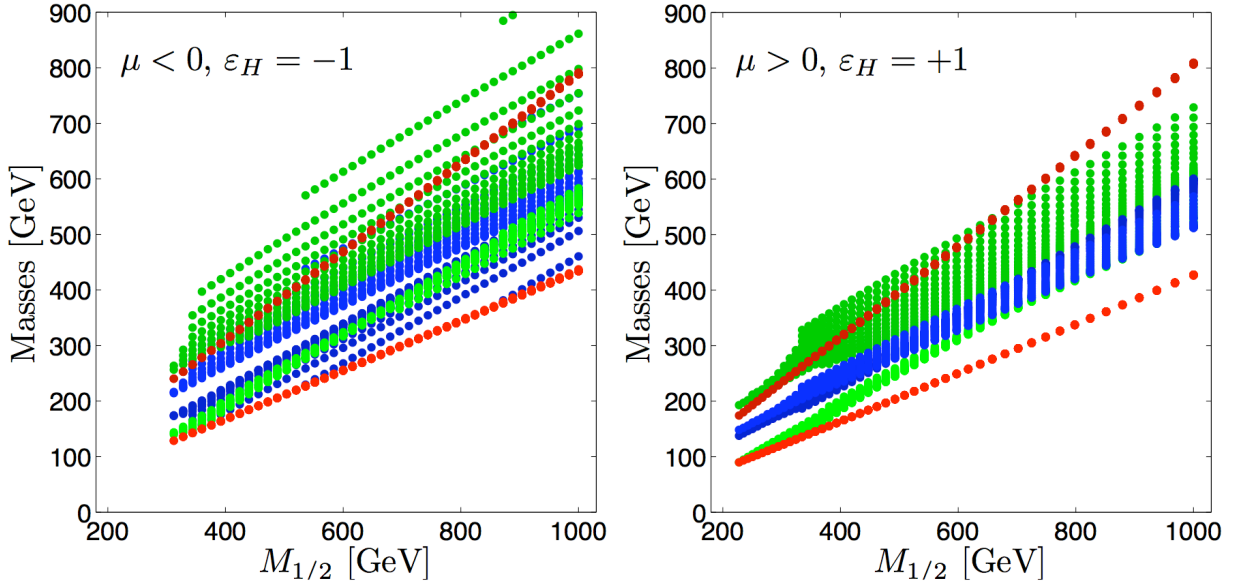


Figure 5: Mass spectrum in the neutralino LSP region, passing LEP and B-physics constraints, as a function of $M_{1/2}$. The colour convention is as follows: red: $\tilde{\chi}_1^0$, green: $\tilde{\tau}_1$, blue: \tilde{e}_R , dark blue: \tilde{e}_L , dark green: $\tilde{\tau}_2$, dark red: $\tilde{\chi}_2^0$.

confirms the result of [18], who did not include the effects of a Chern–Simons term and consequently did not find any viable parameter regions, except for extremely unnatural values for the gaugino masses far above our scan limits. At the same time it is important that c' , which is an $\mathcal{O}(1)$ parameter, never becomes large.

Implications for collider phenomenology can be deduced from Fig. 5, which shows the neutralino and slepton mass spectrum in the neutralino LSP region. We see that the second-lightest neutralino $\tilde{\chi}_2^0$ and the lighter chargino $\tilde{\chi}_1^\pm$, which are mainly winos ($m_{\tilde{\chi}_1^\pm} \simeq m_{\tilde{\chi}_2^0}$), are always heavier than $\tilde{e}_{R,L}$ and $\tilde{\tau}_1$ (with the exception of a few points at $\mu < 0$ which have $m_{\tilde{e}_R} > m_{\tilde{\chi}_2^0} > m_{\tilde{e}_L}$). Note the clear separation of the selectron masses with $m_{\tilde{e}_L} < m_{\tilde{e}_R}$ for $\mu < 0$, while for $\mu > 0$ we have $m_{\tilde{e}_L} \sim m_{\tilde{e}_R}$. The squark and gluino masses are not shown, but they are roughly $m_{\tilde{q}} \sim m_{\tilde{g}} \sim (2-3)M_{1/2}$. At the LHC, squarks and gluinos will hence be produced both as $\tilde{q}\tilde{q}$ or $\tilde{g}\tilde{g}$ pairs, and in $\tilde{q}\tilde{g}$ associated production. Their decays are $\tilde{g} \rightarrow q\tilde{q}_{R,L}$, $\tilde{q}_R \rightarrow q\tilde{\chi}_1^0$, $\tilde{q}_L \rightarrow q'\tilde{\chi}_1^\pm$ or $q\tilde{\chi}_2^0$, as in the mSUGRA scheme with large $|\mu|$ [44]. Moreover, the decays $\tilde{\chi}_2^0 \rightarrow e^\pm\tilde{e}_L^\mp \rightarrow e^+e^-\tilde{\chi}_1^0$ and $\tilde{\chi}_2^0 \rightarrow \tau^\pm\tilde{\tau}_1^\mp \rightarrow \tau^+\tau^-\tilde{\chi}_1^0$ are always open and together have about 50% branching ratio; the other 50% go into neutrinos. This leads to the gold-plated same-flavour opposite-sign (SFOS) dilepton signature at the LHC [45], which allows to reconstruct sparticle masses. Furthermore, the decay of the lighter chargino always leads to a charged lepton, $\tilde{\chi}_1^\pm \rightarrow (\ell^\pm\tilde{\nu}_\ell \text{ or } \nu_\ell\tilde{\ell}^\pm) \rightarrow \ell^\pm\nu_\ell\tilde{\chi}_1^0$, giving rise to a large number of events with jets plus 1 hard lepton plus missing transverse energy, E_T^{miss} . If combined with $\tilde{\chi}_2^0 \rightarrow \dots \rightarrow l^+l^-\tilde{\chi}_1^0$, this leads to the rather clean trilepton signature (plus jets plus E_T^{miss}).

The scenario becomes even more predictive if we require that the neutralino LSP have a relic density in agreement with cosmological observations (assuming standard cosmology). Imposing the 3σ upper bound from WMAP5, $\Omega h^2 < 0.1285$, constrains $M_{1/2} \lesssim 390$ GeV with $\tan\beta \gtrsim 11$ for $\mu > 0$. For $\mu < 0$, it gives an upper limit on $M_{1/2}$ which increases with $\tan\beta$, from $M_{1/2} \lesssim 312$ GeV at $\tan\beta = 12$ to $M_{1/2} \lesssim 920$ GeV at $\tan\beta = 20$. The

reason is that the LSP is almost a pure bino and has a small pair-annihilation cross section (s-channel Higgs exchange is not efficient in this scenario); in order to have a small enough relic density, the LSP needs to co-annihilate with another sparticle which is close in mass, typically the next-to-lightest SUSY particle (NLSP). This constrains the scenario to the region of small NLSP–LSP mass differences near the boundary to the slepton LSP region, which is realized for $\mu < 0$ up to large $M_{1/2}$ (depending on $\tan\beta$), but for $\mu > 0$ only at small $M_{1/2}$, cf. Figs. 3 and 5. Note, however, that this is a direct consequence of the simplified assumptions for the matter sector.

7 Realistic sfermion soft terms

In this section we explain how improved sfermion soft terms can be obtained if we model the matter sector as in the Burdman–Nomura model [12]. The third generation matter fields arise from the mixing of brane and bulk fields. Bulk fields with flat profile have Yukawa couplings determined by the 5d gauge coupling. Non-trivial bulk profiles cause a reduced overlap with the Higgs wave function and hence smaller Yukawa couplings. Thus, using both bulk masses and mixing angles we can obtain realistic values for y_t , y_b and y_τ .

For the third generation quarks in particular, we introduce a 5d bulk hypermultiplet $\{\mathcal{U}, \mathcal{U}^c\}$ in the **20** of SU(6) containing as 4d zero modes the right-handed top quark superfield and a weak doublet, and another bulk hypermultiplet $\{\mathcal{D}, \mathcal{D}^c\}$ in the **15** containing the right-handed bottom quark and a second doublet. We give these fields bulk masses M_u and M_d . Furthermore, brane-localized superfields must be introduced to decouple unwanted massless fields. They couple to the doublet components of both the \mathcal{U} and \mathcal{D} fields, leaving a single massless quark doublet instead of the two we were starting with. This effect is parametrized by a mixing angle ϕ_Q .

Similarly, leptons descend from two 5d bulk hypermultiplets, $\{\mathcal{E}, \mathcal{E}^c\}$ in the **15** and $\{\mathcal{N}, \mathcal{N}^c\}$ in the **6**. In analogy with the quark sector this leads to three more model parameters, two bulk masses M_e and M_n and a mixing angle ϕ_L . For details of the model, in particular for the proper choice of boundary conditions, brane fields and bulk-brane couplings, we refer to [12].

The kinetic functions are computed by integrating the zero-mode profiles over the fifth dimension, replacing its radius R by $(T + \bar{T})/2$. This gives

$$Y_{U_3} = \frac{1}{2|M_u|} \left(1 - e^{-\pi(T+\bar{T})|M_u|}\right), \quad (37)$$

$$Y_{Q_3} = \frac{1}{2|M_u|} \left(1 - e^{-\pi(T+\bar{T})|M_u|}\right) \sin^2(\phi_Q) + \frac{1}{2|M_d|} \left(1 - e^{-\pi(T+\bar{T})|M_d|}\right) \cos^2(\phi_Q), \quad (38)$$

$$Y_{D_3} = \frac{1}{2|M_d|} \left(1 - e^{-\pi(T+\bar{T})|M_d|}\right). \quad (39)$$

The kinetic functions for the lepton sector are obtained in the same manner, and are given by the same expressions with the obvious parameter replacements. The soft masses and A -terms are then derived from Eqs. (25) – (27). We refrain from giving closed-form expressions for them, since these are rather cumbersome and not very illuminating.

The parameters $M_u, M_d, M_n, M_e, \phi_Q$ and ϕ_L cannot be chosen entirely freely, because they also have to account for the proper physical values of the Yukawa and gauge couplings.

Since the Higgs wave function normalization is just given by $\langle Y_H \rangle = 1/g_4^2$ and in particular is independent of c' , the relations given in [12] apply:¹²

$$y_t = \sin(\phi_Q) \frac{\pi R |M_u|}{\sinh \pi R |M_u|} g_4, \quad y_b = \cos(\phi_Q) \frac{\pi R |M_d|}{\sinh \pi R |M_d|} g_4, \quad (40)$$

$$y_n = \sin(\phi_L) \frac{\pi R |M_n|}{\sinh \pi R |M_n|} g_4, \quad y_\tau = \cos(\phi_L) \frac{\pi R |M_e|}{\sinh \pi R |M_e|} g_4. \quad (41)$$

In the numerical analysis, in order to avoid additional model dependence from the unknown neutrino sector, we will assume that M_n is large enough not to contribute to the stau soft terms. We also introduce a Majorana mass term for the right-handed neutrinos on the $y = 0$ brane as in [12]. Since M_n is large, the neutrino wave function will be strongly localized towards the $y = \pi R$ brane, resulting in an exponentially suppressed Yukawa coupling and a doubly exponentially suppressed Majorana mass. The suppression factors will cancel out in the see-saw formula for the lighter neutrino mass eigenstate, leading to the same lighter neutrino mass as in the standard see-saw mechanism. The heavier neutrino mass, on the other hand, will be lowered by a factor $\sim e^{-4\pi R |M_n|}$ with respect to the GUT scale. This may be beneficial for leptogenesis [46].

It is instructive to see how Eq. (40) constrains the possible ranges of squark soft terms. In the remainder of this section we will therefore give some estimates of the bounds on the squark masses and trilinear couplings.

For $\tan \beta \sim 5-50$, the relevant GUT-scale Yukawa couplings take values $0.5 \lesssim y_t \lesssim 0.6$ and $0.02 \lesssim y_b \lesssim 0.3$. We also know that the gauge couplings unify at $g_4 \approx 0.7$.

To reproduce the top Yukawa coupling, we must have $\tan \phi_Q \gtrsim 1$ by Eq. (40). The small ratio y_b/y_t can then be generated either by choosing $\tan \phi_Q$ to be large, or choosing $|M_d| > |M_u|$, or by a combination of these. The relation between M_u , M_d , ϕ_Q and the Yukawa couplings is illustrated in Fig. 6. We note that for given y_t and y_b , the allowed range for the mixing angle ϕ_Q is

$$\phi_Q = [\arcsin(y_t/g_4), \arccos(y_b/g_4)]. \quad (42)$$

For estimating the size of the squark-mass parameters, let us consider two limiting cases:

- If the difference between y_t and y_b is mainly due to the different bulk masses, then $\tan \phi_Q \approx 1$. This corresponds to the far left region of Fig. 6. In that case $\sin \phi_Q \approx 1/\sqrt{2}$ already accounts for the ratio $y_t/g_4 \approx 0.7$ in Eq. (40). The top Yukawa coupling should thus not receive much additional suppression from large bulk masses, hence we need $|M_u| \ll 1/R$. Expanding Eq. (37) and retaining only the leading term, we reproduce Y_{U_3} as in Eq. (34):

$$Y_{U_3} = \frac{\pi}{2} (T + \bar{T}), \quad m_{U_3}^2 = \left| \frac{F^T}{2R} \right|^2. \quad (43)$$

On the other hand, $R|M_d|$ must be sizeable to obtain an appropriately suppressed y_b , cf. Fig. 6. With Eq. (39), $m_{D_3}^2$ turns out to be

$$m_{D_3}^2 = \left(\frac{\pi R |M_d|}{\sinh(\pi R |M_d|)} \right)^2 \left| \frac{F^T}{2R} \right|^2 \approx 4y_b^2 \left| \frac{F^T}{2R} \right|^2. \quad (44)$$

¹²Note that our conventions for ϕ_Q and ϕ_L slightly differ from those of [12].

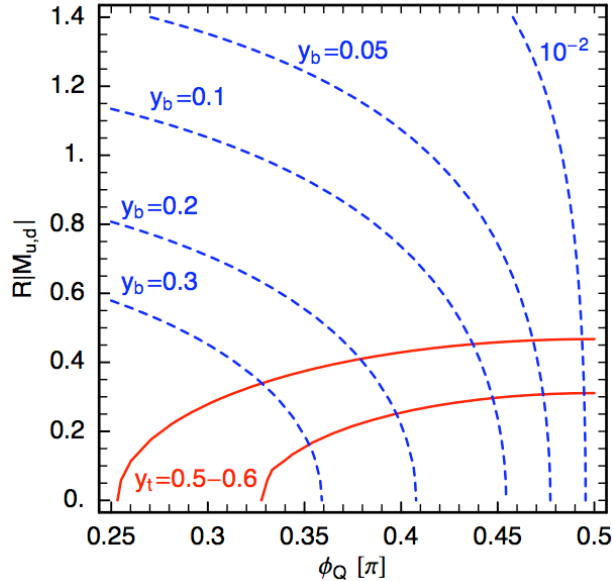


Figure 6: Values of $R|M_u|$ and $R|M_d|$ as function of the mixing angle ϕ_Q for various values of y_t (full red lines) and y_b (dashed blue lines). Note that y_t gives the lower and y_b the upper bound of the allowed range of ϕ_Q .

Finally, the quark doublet soft mass-squared $m_{Q_3}^2$ obtained from Eq. (38) is numerically

$$m_{Q_3}^2 \approx (0.7 - 0.8) \times \left| \frac{F^T}{2R} \right|^2. \quad (45)$$

- If $\tan \phi_Q \gg 1$, i.e. $\sin \phi_Q \approx 1$ (which is the case in the far right region of Fig. 6), then the ratio $y_t/g_4 \approx 0.7$ is mainly due to a sizeable bulk mass M_u . Numerically, we need $R|M_u| \approx 0.3 - 0.5$. Therefore we should use the full expression for Y_{U_3} , rather than just the leading term:

$$m_{U_3}^2 = \left(\frac{\pi R|M_u|}{\sinh(\pi R|M_u|)} \right)^2 \left| \frac{F^T}{2R} \right|^2 \approx (0.5 - 0.8) \times \left| \frac{F^T}{2R} \right|^2. \quad (46)$$

Dropping the $\cos^2 \phi_Q$ piece in Y_{Q_3} and setting $\sin \phi_Q = 1$, we obtain the same expression for Y_{Q_3} and eventually $m_{Q_3}^2$:

$$m_{Q_3}^2 = \left(\frac{\pi R|M_u|}{\sinh(\pi R|M_u|)} \right)^2 \left| \frac{F^T}{2R} \right|^2 \approx (0.5 - 0.8) \times \left| \frac{F^T}{2R} \right|^2. \quad (47)$$

As is evident from Fig. 6, if y_b is to remain finite, $\tan \phi_Q$ cannot become arbitrarily large. In any case, this limit requires very small y_b . The constraints on $|M_d|R$ are rather weak, although smaller $|M_d|R$ is somewhat favoured in order not to get additional y_b suppression. Hence

$$m_{D_3}^2 \lesssim \left| \frac{F^T}{2R} \right|^2. \quad (48)$$

In the end we expect the squark masses-squared to lie somewhere in between these two extremes:

$$0.5 \times \left| \frac{F^T}{2R} \right|^2 \lesssim (m_{Q_3}^2, m_{U_3}^2) \lesssim \left| \frac{F^T}{2R} \right|^2, \quad 0 \lesssim m_{D_3}^2 \lesssim \left| \frac{F^T}{2R} \right|^2. \quad (49)$$

In order to obtain limits on A_t , we can make the same case distinction:

- for $\tan \phi_Q \approx 1$ and small $|M_u|$, we get

$$A_t \approx \frac{F^T}{2R} \left(-\frac{1+2c'}{1+c'} + 1 + \frac{2\pi R|M_d| (1 + e^{-2\pi R|M_d|})}{2\pi R|M_d| + 1 - e^{-2\pi R|M_d|}} \right); \quad (50)$$

- for $\sin \phi_Q \approx 1$, we obtain

$$A_t \approx \frac{F^T}{2R} \left(-\frac{1+2c'}{1+c'} + 2 \frac{2\pi R|M_u|}{\exp(2\pi R|M_u|) - 1} \right). \quad (51)$$

Numerically,

$$A_t \approx \frac{F^T}{2R} \left(-\frac{1+2c'}{1+c'} + \alpha \right) \quad (52)$$

where $0.3 \lesssim \alpha \lesssim 2$, with $\alpha = 2$ corresponding to the first of the above two cases (with $R|M_d| \approx 1$), and $\alpha = 0.3$ to the second (with $R|M_u| = 0.5$). Evidently A_t can take a wide range of values, significantly departing from the simplified case of Section 6. In particular it can become large and negative, which will be of relevance in the next Section. A similar statement turns out to be true for A_b , for which we find an analogous estimate with $0 \lesssim \alpha \lesssim 1.4$.

8 Results for realistic sfermion soft terms

Let us finally investigate to what extent the phenomenological features found in Section 6 remain valid when invoking realistic stop, sbottom and stau parameters derived from the Burdman–Nomura model. The six new parameters $M_u, M_d, M_n, M_e, \phi_Q, \phi_L$ are subject to four constraints, since they are related to the Yukawa couplings according to Eqs. (40) and (41). As detailed above we assume that M_n is large enough not to affect the stau soft terms. This corresponds to a negligible neutrino Yukawa coupling, and we do not need to worry about lepton flavour violation [47]. The precise value of M_n is irrelevant. (If M_n did contribute to the stau soft terms, its main effect would be to increase m_{L_3} , thus rendering the staus heavier, but leaving the overall picture intact.) We are therefore left with five parameters, $M_{u,d,e}$ and $\phi_{Q,L}$, and three constraints from y_t, y_b and y_τ .

We choose ϕ_Q and ϕ_L as the two independent new parameters and scan the parameter space as in Section 6, with the following modifications:

- We vary $M_{1/2}$ from 100 to 1000 GeV, ϕ_Q from $\pi/4$ to $\pi/2$, and ϕ_L from 0 to $\pi/2$. For $\tan \beta$, we consider three distinct values, $\tan \beta = 10, 20$, and 30 , in order to avoid excessive computing times.

- For each point, the bulk masses $M_{u,d,e}$ are computed from the GUT-scale gauge and Yukawa couplings g_4, y_t, y_b, y_τ by numerically inverting Eqs. (40) and (41). They then serve as input in the kinetic functions Eqs. (37)–(39), and the analogous expressions for the leptons, from which the sfermion soft masses and A -terms are obtained according to Eqs. (25)–(27). The soft terms of the first and second generation are again assumed to be zero at the GUT scale.

The result of this scan is shown in Figs. 7 and 8 for the two signs of μ . For better readability, we only show $M_{1/2}$ in steps of 200 GeV, although the scan had a much finer grid. Contrary to the case of simplified boundary conditions, now μ and ϵ_H need to be of opposite sign. The reason is that now A_t turns out to be negative at the GUT scale (cf. the discussion in Section 4).

It is interesting to see how the mixing angles ϕ_Q and ϕ_L influence the nature of the LSP. ϕ_L determines the size of the stau parameters. Since it is constrained by the tau Yukawa coupling it can only vary over a sizable range if $\tan\beta$ is large. The reason is that A_τ is generically large, leading to a charge-breaking minimum if m_{L_3, E_3} are too small. Thus for $\tan\beta \sim 10$, ϕ_L is close to $\pi/2$ and the staus are rather heavy compared to the selectrons. For larger $\tan\beta$ (i.e. larger y_τ), ϕ_L can be small and the $\tilde{\tau}_1$ can become the LSP, corresponding to the green points in Figs. 7 and 8. Note, however, that the stau LSP region is highly constrained by direct mass bounds and B -physics, and that a stable LSP is excluded by cosmology. ϕ_L also has some effect on the selectron masses through RG evolution, but this is much less pronounced.

The angle ϕ_Q , on the other hand, determines the size of the stop and sbottom parameters. Through RG evolution it also influences the slepton masses, in particular $m_{\tilde{e}_R}$: larger ϕ_Q leads to a larger m_{D_3} , which in turn decreases $m_{\tilde{e}_R}$. In Figs. 7 and 8 one can see clearly that for increasing ϕ_Q , the \tilde{e}_R eventually becomes the LSP. This behaviour can be understood easily from the $U(1)_Y$ D -term contribution to the evolution of the scalar soft masses m_i^2 [48]. At one loop

$$\frac{d}{dt}m_i^2 \sim \frac{6}{5} \frac{g_1^2 Y_i}{16\pi^2} S, \quad (53)$$

where Y_i is the weak hypercharge and

$$S = (m_{H_2}^2 - m_{H_1}^2) + \text{Tr} (m_Q^2 - 2m_U^2 + m_D^2 + m_R^2 - m_L^2) \quad (54)$$

with the trace running over generations. Since S is an RG invariant, it simply causes a shift of the low-scale masses by $\Delta m_i^2 \approx -(0.052) Y_i S_{\text{GUT}}$ [49] with respect to the values they would have had for $S \equiv 0$. Here S_{GUT} is the value of S at M_{GUT} . For simplified boundary conditions, we had $S_{\text{GUT}} = -m_{U_3}^2$. With $Y_{e_R} = 1$ and $Y_{e_L} = -1/2$, making S_{GUT} less negative obviously lowers $m_{\tilde{e}_R}$ and increases $m_{\tilde{e}_L}$ (note also that the effect for the left-chiral state is only half the size of that for the right-chiral one). Moreover, comparing $m_{\tilde{e}_R} \approx (0.39 M_{1/2})^2 - 0.052 S_{\text{GUT}}$ to $m_{\tilde{\chi}_1^0} \approx 0.43 M_{1/2}$, we understand why the \tilde{e}_R eventually becomes the LSP.

The projections onto the underlying model parameters $F^T/2R$, F^φ and c' are shown in Fig. 9. Since here we need $\text{sign}(\mu) = -\epsilon_H$ to obtain a valid spectrum, F^φ now turns out to be small and can even be zero. Contributions to the soft terms from anomaly mediation are therefore completely negligible. Moreover, we find a somewhat smaller range for the c' parameter, roughly $0.5 \lesssim c' \lesssim 1.2$, as compared to $0.5 \lesssim c' \lesssim 3$ for simplified boundary

conditions. The important point, however, is that c' remains non-zero. We conclude that the Chern–Simons term is indeed essential to achieve correct EWSB.

Let us now turn to the implications for collider phenomenology. We again focus on the neutralino LSP region. The mass spectrum in this region, taking into account the constraints from LEP and from B-physics, is depicted in Fig. 10. As one can see, there is a definite mass ordering $m_{\tilde{\chi}_1^\pm} \simeq m_{\tilde{\chi}_2^0} > m_{\tilde{e}_L} > m_{\tilde{e}_R} > m_{\tilde{\chi}_1^0}$. The $\tilde{\tau}_2$ turns out to be heavier than the $\tilde{\chi}_2^0$, while the $\tilde{\tau}_1$ can be lighter than the $\tilde{\chi}_2^0$, and for small ϕ_L also lighter than the selectrons, cf. the above discussion of the mixing-angle dependence. This gives a picture that is qualitatively similar to the simplified case discussed in Section 6; the main difference lies in the masses and mass ratios of the sleptons. For the squarks, this effect of non-universality — on the one hand the splitting of the third generation from the first and second generations due to non-zero m_{Q_3, U_3, D_3}^2 , on the other hand the splitting of left- and right-chiral states due to non-zero S — is much less pronounced, because the running of the squark mass parameters is mainly driven by M_3 . The squark and gluino masses are hence again about $m_{\tilde{q}} \approx m_{\tilde{g}} \approx (1.7 - 2.5)M_{1/2}$. The masses of the higgsino-like neutralinos and chargino are given by $|\mu|$ and lie above $m_{\tilde{g}}$.

It is also remarkable that now the neutralino relic density can vary over a large range, because of the extra parameters ϕ_Q and ϕ_L . This is illustrated in Fig. 11 for the example of $M_{1/2} = 500$ GeV and two values of $\tan\beta$ for each sign of μ . For $\mu > 0$, we take $\tan\beta = 10$ and 30; for $\mu < 0$, we take $\tan\beta = 10$ and 20 since higher values are too tightly constrained. The figure compares the neutralino relic density Ωh^2 , as a function of ϕ_Q and ϕ_L , with the WMAP5 observation at 3σ . In the orange regions Ωh^2 is too low, which would require other constituents of dark matter in addition to the neutralino. In the brown regions, on the other hand, Ωh^2 is too high (at least within standard cosmology; it could be viable if there was, e.g., additional entropy production after freeze-out). The minimal and maximal values found are $\Omega h^2 \simeq 6 \times 10^{-3}$ and 0.9, respectively. In the red band in between, however, $0.0913 \leq \Omega h^2 \leq 0.1285$ agrees within 3σ with the value measured by WMAP5. The reason is that here the mass difference between the LSP and NLSP (or co-NLSPs) is just right to make co-annihilation processes efficient enough, but not too efficient, to obtain $\Omega h^2 \simeq 0.1$. To be precise, in the red bands of Fig. 11 we typically have $\Delta m = m_{\tilde{e}_R} - m_{\tilde{\chi}_1^0} \simeq 7 - 10$ GeV. An exception is $\mu > 0$, $\tan\beta = 30$ and small ϕ_L , where the $\tilde{\tau}_1$ becomes light and also contributes to co-annihilations, such that $\Delta m \approx 20$ GeV is needed; this leads to the red band bending down towards lower ϕ_Q . Sample spectra of five representative points, indicated as points A–E in Fig. 11, are given in Tables 1 and 2. Table 1 gives GUT and EWSB scale parameters, and Table 2 lists the resulting masses together with B-physics observables, the neutralino relic density and the neutralino–proton scattering cross section for direct detection. The possibility to tune the NLSP–LSP mass difference by adjusting ϕ_Q and ϕ_L and to obtain the correct relic density persists also for other values of $M_{1/2}$.

To summarize, the expected LHC phenomenology is as follows:

- Squarks and gluinos with masses up to about 2 TeV will be abundantly produced at the LHC, both as $\tilde{q}\tilde{q}$ or $\tilde{g}\tilde{g}$ pairs, and in $\tilde{q}\tilde{g}$ associated production. They decay as $\tilde{g} \rightarrow q\tilde{q}_{R,L}$, $\tilde{q}_R \rightarrow q\tilde{\chi}_1^0$ ($\sim 100\%$), $\tilde{q}_L \rightarrow q'\tilde{\chi}_1^\pm$ ($\sim 65\%$) or $q\tilde{\chi}_2^0$ ($\sim 30\%$).
- The decay $\tilde{\chi}_2^0 \rightarrow e^\pm\tilde{e}_L^\mp \rightarrow e^+e^-\tilde{\chi}_1^0$ is always open and has a sizable branching ratio ($\sim 45\%$ for points A–D, 35% for point E). This leads to a rather large rate for the gold-

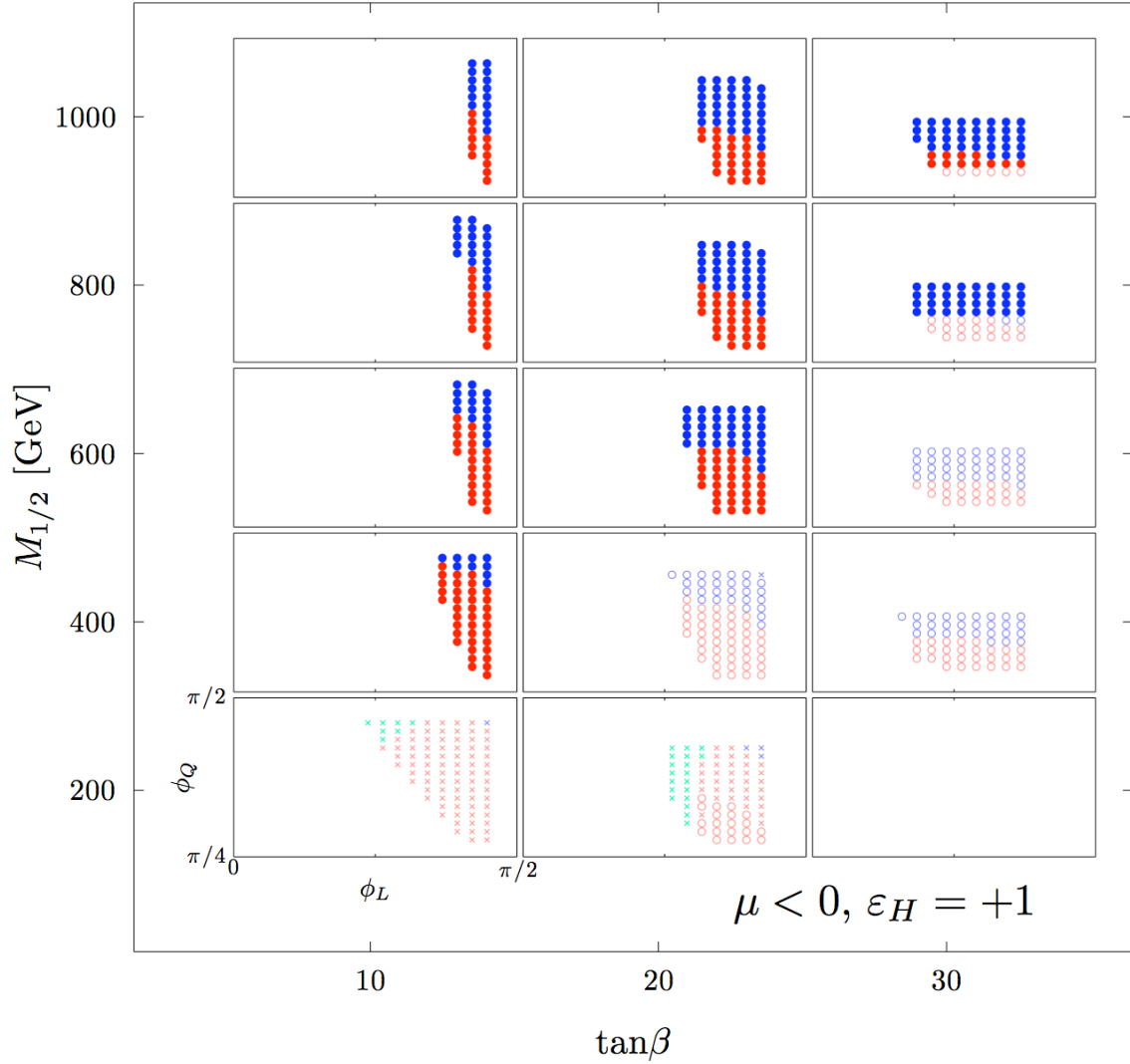


Figure 7: Points which lead to correct EWSB from a scan over $M_{1/2}$, $\tan\beta$, ϕ_Q and ϕ_L , for $\mu < 0$, $\epsilon_H = +1$ and sfermion soft terms determined according to the Burdman–Nomura model. Small crosses denote points excluded by LEP, while open circles denote points excluded by B -physics constraints. Points passing these constraints are shown as big full dots. The colours denote the nature of the LSP: red, green and blue points have a neutralino, stau and selectron LSP, respectively.

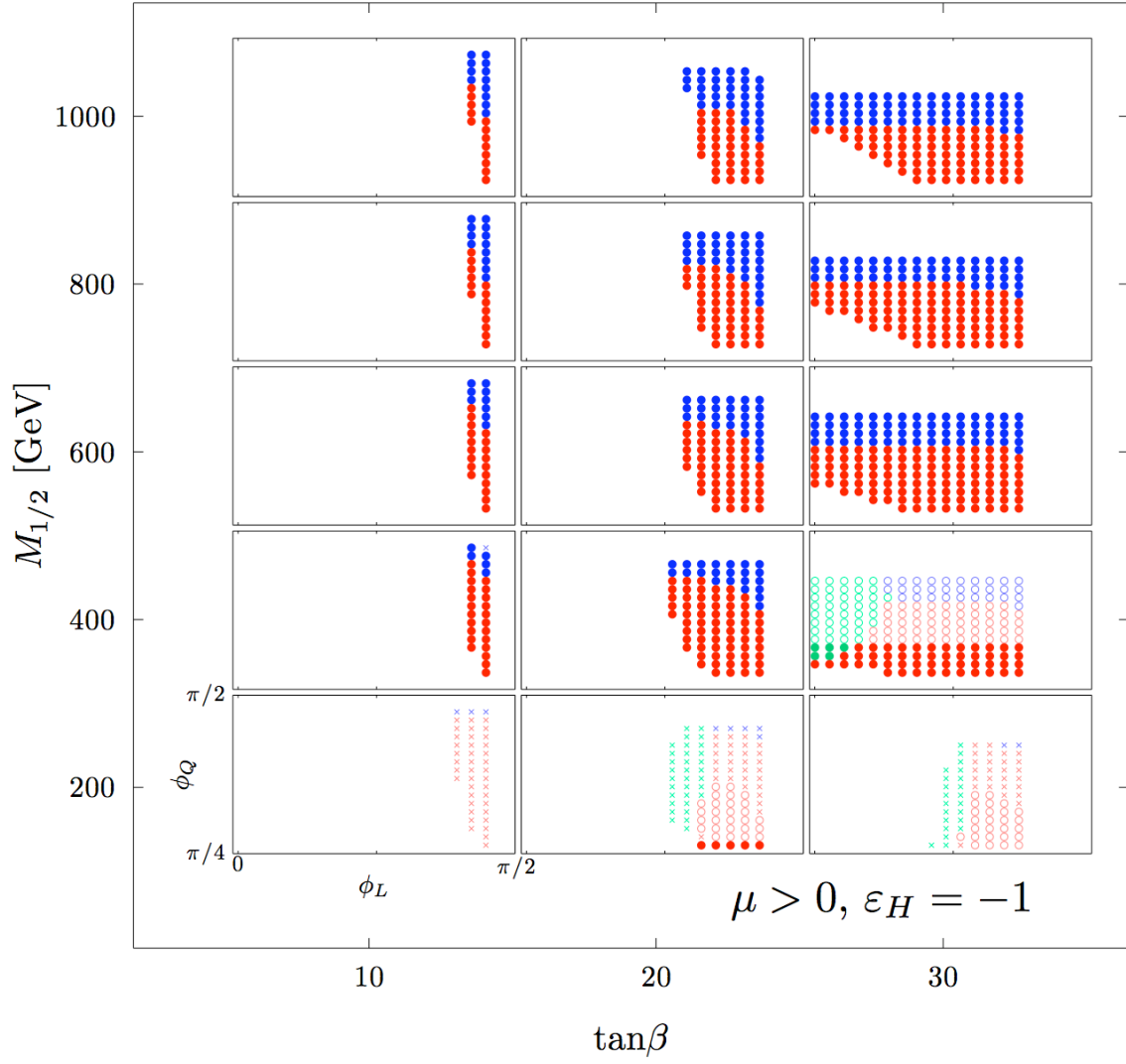


Figure 8: Same as Fig. 7 but for $\mu > 0$ and $\epsilon_H = -1$.

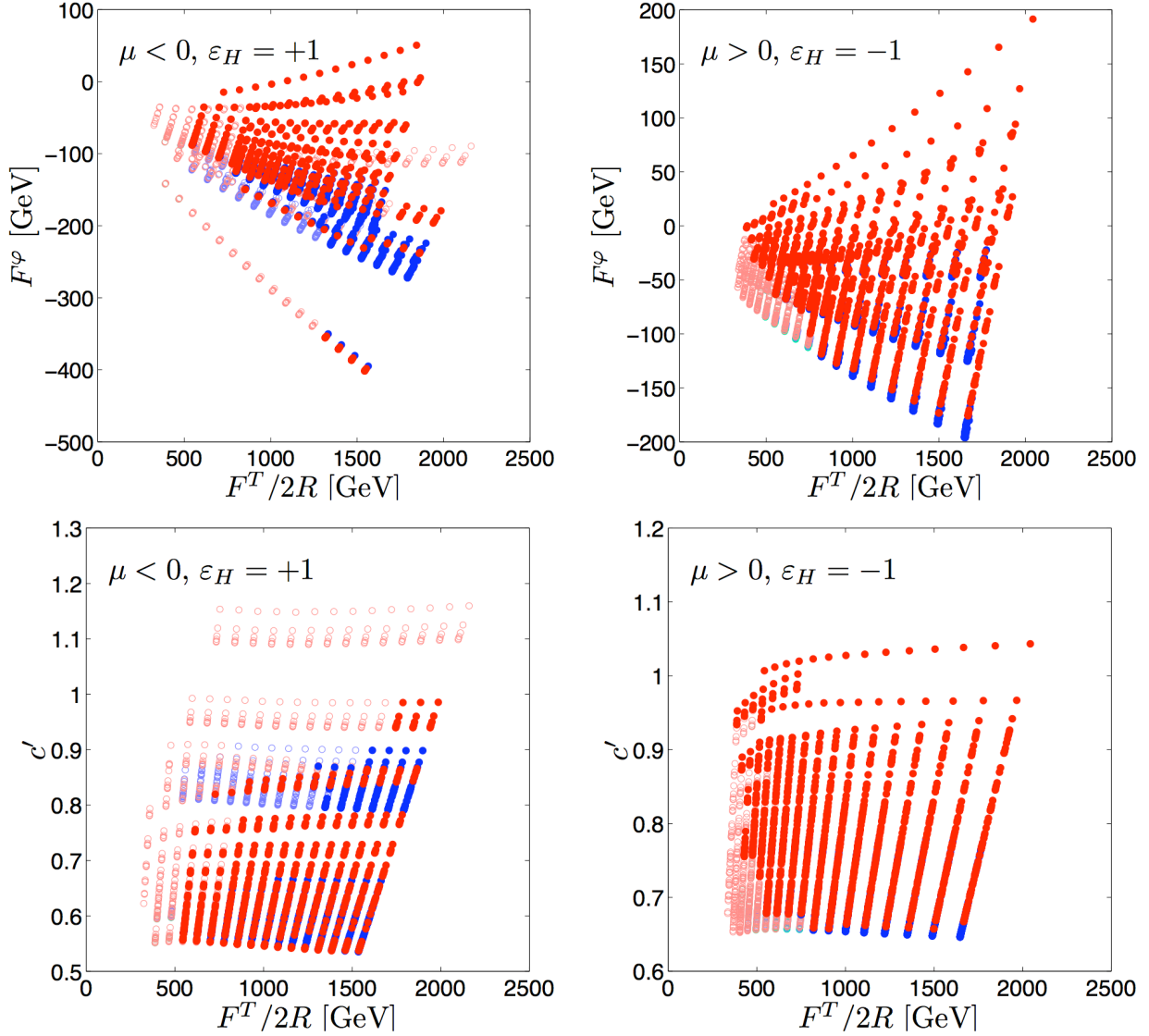


Figure 9: Points of Figs. 7 and 8 in the $F^T/2R$ vs. F^φ plane (top row) and in the $F^T/2R$ vs. c' plane (bottom row). The red, green and blue points have a neutralino, stau and selectron LSP, respectively. Open circles denote points excluded by B-physics constraints. Points excluded by LEP are not shown.

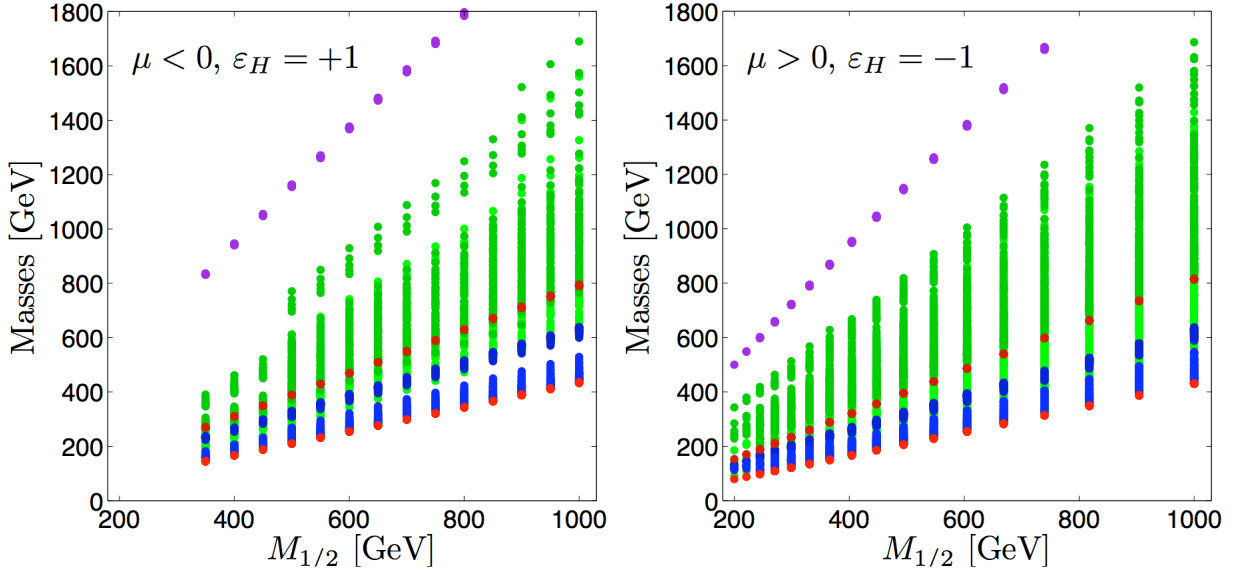


Figure 10: Mass spectrum in the neutralino LSP region, passing LEP and B-physics constraints, as a function of $M_{1/2}$. From bottom to top: $\tilde{\chi}_1^0$ (red), \tilde{e}_R (blue), \tilde{e}_L (dark blue), $\tilde{\tau}_1$ (green), $\tilde{\chi}_2^0$ (dark red), $\tilde{\tau}_2$ (dark green) and \tilde{g} (purple).

plated SFOS dilepton signature. In parts of the parameter space, also $\tilde{\chi}_2^0 \rightarrow \tau^\pm \tilde{\tau}_1^\mp \rightarrow \tau^- \tau^+ \tilde{\chi}_1^0$ can be kinematically allowed; c.f. point E, where it has 22% branching ratio. Decays into Z , h , or \tilde{e}_R are negligible because the $\tilde{\chi}_2^0$ is almost a pure wino.

- The decay of the $\tilde{\chi}_1^\pm$ always leads to a charged lepton, $\tilde{\chi}_1^\pm \rightarrow \ell^\pm \tilde{\nu}_\ell / \nu_\ell \tilde{\ell}_L^\pm \rightarrow \ell^\pm \nu_\ell \tilde{\chi}_1^0$, giving rise to a large number of events with jets plus one hard lepton plus E_T^{miss} . If combined with $\tilde{\chi}_2^0 \rightarrow \dots \rightarrow l^+ l^- \tilde{\chi}_1^0$ on the other side of the event, it leads to the rather clean tripleton signature (plus jets plus E_T^{miss}).
- The higgsino states $\tilde{\chi}_{3,4}^0$ and $\tilde{\chi}_2^\pm$ have masses around or above the gluino mass and are hence too heavy to be studied at the LHC.

Overall the scenario resembles the mSUGRA/CMSSM case with small m_0 , or the case of Higgs boson exempt no-scale supersymmetry (HENS) [49]. An important difference are the sizeable third-generation high-scale soft terms which our construction predicts. Ways to distinguish between the different models include, e.g., the rate of leptonic events, which is expected to be higher in our scenario as compared to the mSUGRA case with the same $M_{1/2}$. Other distinctive features are the ratios of left- and right-chiral slepton masses and the non-universality of the third generation.¹³ Note, however, that the \tilde{e}_R does not couple to the wino-like $\tilde{\chi}_2^0$ and $\tilde{\chi}_1^\pm$ and hence does not appear in decay chains at the LHC. The \tilde{e}_R is therefore best studied in e^+e^- collisions, as are the staus if they are too heavy to be produced in $\tilde{\chi}_2^0$ decays.

Last but not least, a decisive test of GHU requires the precise measurement of the complete spectrum, including stops, sbottoms, heavy Higgs bosons and higgsinos, such that the SUSY Lagrangian parameters can be extracted and a bottom-up evolution along

¹³We leave a detailed study of characteristic mass ratios and model footprints for future work.

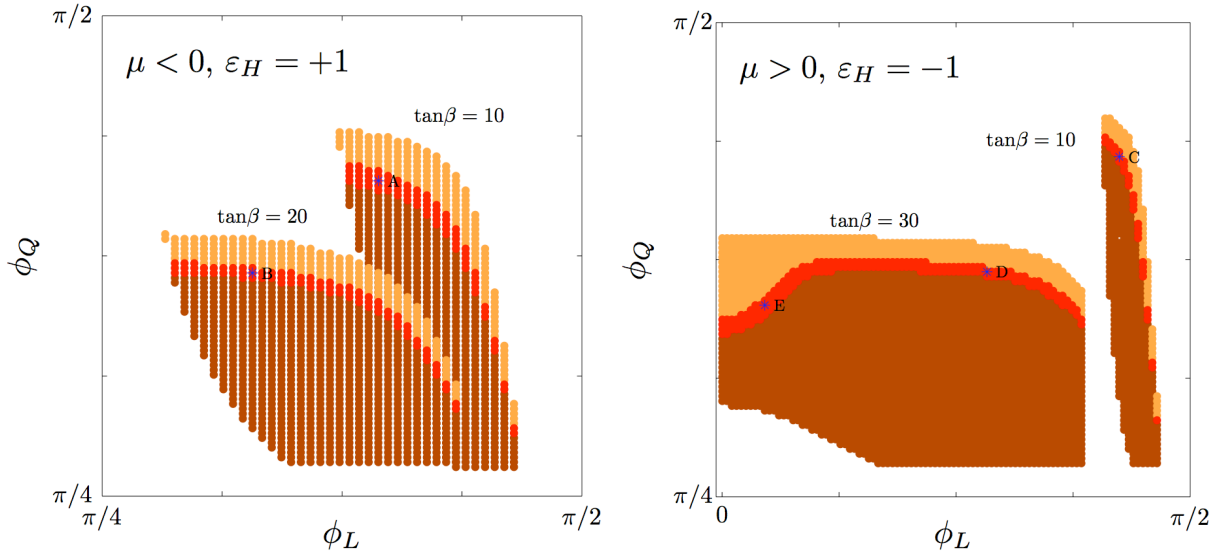


Figure 11: Dependence of the neutralino relic density on the mixing angles ϕ_Q and ϕ_L , for $M_{1/2} = 500$ GeV and various values of $\tan\beta$. In the red bands, Ωh^2 lies within 3σ of the WMAP5 observation, $0.0913 < \Omega h^2 < 0.1285$. In the orange regions, $\Omega h^2 < 0.0913$ is too low, while in the brown regions $\Omega h^2 > 0.1285$ is too high. Also indicated are the sample points A–E.

the lines of [50] performed. This can only be achieved at a (multi-)TeV e^+e^- linear collider with a very good beam performance.

9 Conclusions

We have investigated SUSY grand unified models with gauge-Higgs unification (GHU). A particularly interesting class of such models are 5d orbifold GUTs and heterotic string models which admit a 5d orbifold GUT limit. With the natural assumption of radion mediation, GHU models are quite predictive as far as the Higgs sector is concerned. The GUT-scale Higgs mass parameters are subject to the GHU relations, and are also tied to the gaugino mass. Despite these strong constraints, models of this type can be fully realistic, as we have shown. If the effects of a Chern–Simons term (which is generically present in 5d models) are taken into account, one finds regions in the parameter space which lead to proper electroweak symmetry breaking and satisfy the experimental bounds from direct Higgs and superpartner searches, rare decays and cosmology. We demonstrated this by using a variation of a 5d SU(6) orbifold GUT model due to Burdman and Nomura as a concrete example. We gave detailed expressions for the soft SUSY breaking parameters in terms of the fundamental model data, including the Chern–Simons term.

Using the high-scale relations between soft terms and estimates of running effects, we discussed qualitatively which parts of the parameter space might be promising. We then presented a detailed numerical analysis of the corresponding RGEs. This analysis was done in two parts, the first for a simplified model of the sfermion sector, and the second treating the relevant sfermion contributions properly as in the Burdman–Nomura model. The latter part of the analysis, while more realistic, is more involved because it depends

on more parameters. In both cases we indeed find viable solutions to the RGEs, satisfying all present experimental constraints. A non-zero Chern–Simons term is essential to get a valid spectrum.

We extracted some characteristic experimental signatures of this class of models, which will be tested at the LHC. In particular, selectrons are generically predicted to be lighter than the $\tilde{\chi}_2^0$, leading to a rather large rate for same-flavour opposite-sign dileptons over the whole parameter space. Higgsinos, on the other hand, are expected to be heavy, presumably beyond the reach of the LHC. Characteristic mass ratios could be tested in detail at a future e^+e^- linear collider.

The LHC will have the potential to narrow down the allowed region in the parameter space of GHU models significantly, or to rule them out. This applies even more to a future linear collider. It would be worthwhile to study in detail how well the scenario discussed here could be reconstructed at the LHC and a linear e^+e^- collider, thereby testing the GHU relation. To this end we proposed a set of benchmark points which may be useful for Monte Carlo simulations.

Acknowledgments

We would like to thank B. Allanach, D. Cerdeño, C. Durnford, J.-L. Kneur, M. Ratz and K. Schmidt-Hoberg for useful discussions. FB thanks the Physik-Department T30e of TU Munich for hospitality and support during the early stages of this project. This work is also supported by the French ANR project ToolsDMColl, BLAN07-2-194882.

Point	A	B	C	D	E
$M_{1/2}$	500	500	500	500	500
$\tan\beta$	10	20	10	30	30
$\text{sign}(\mu)$	-1	-1	+1	+1	+1
ε_H	+1	+1	-1	-1	-1
ϕ_Q	1.3011	1.1503	1.3486	1.1582	1.1027
ϕ_L	1.2376	1.0314	1.3329	0.8889	0.1437
c'	0.5712	0.6118	0.7577	0.6686	0.6811
$F^T/2R$	785.6	805.9	878.9	834.3	840.9
F^φ	-107.7	-120.6	-38.9	-114.6	-109.9
Parameters at M_{GUT}					
μ	-1178.9	-1232.4	1296.6	1283.2	1291.0
B	-344.0	-381.3	-298.0	-393.2	-390.2
m_{U_3}	564.8	615.2	622.9	634.9	657.3
m_{D_3}	239.5	371.2	279.5	413.9	369.2
m_{Q_3}	555.5	592.4	615.9	613.5	626.3
A_t	-812.6	-793.7	-980.0	-842.2	-823.1
A_b	-932.3	-923.6	-1105.6	-966.3	-978.8
m_{R_3}	226.7	304.9	364.1	432.6	278.8
m_{L_3}	161.8	269.4	225.2	407.9	278.5
A_τ	-1055.8	-1073.7	-1216.8	-1070.4	-1149.6
Parameters at M_{EWSB}					
μ	-1217.6	-1238.8	1342.0	1275.3	1282.9
B	-46.8	-16.7	45.9	11.4	10.6
m_1^2	554195	405781	598972	428198	401063
m_2^2	2022	-2969	2560	-3429	-3467

Table 1: Parameters of sample points A–E in Fig. 11. Dimensionful quantities are in GeV, $B \equiv B\mu/\mu$.

Point	A	B	C	D	E
$m_{\tilde{\chi}_1^0}$	210.1	210.3	208.1	208.7	208.7
$m_{\tilde{\chi}_2^0}$	389.3	389.5	399.2	400.4	400.3
$m_{\tilde{\chi}_3^0}$	1219.7	1240.7	1332.0	1265.2	1272.8
$m_{\tilde{\chi}_4^0}$	1220.3	1241.9	1335.1	1267.7	1275.3
$m_{\tilde{\chi}_1^\pm}$	389.3	389.4	399.2	400.4	400.3
$m_{\tilde{\chi}_2^\pm}$	1222.8	1244.1	1335.4	1268.4	1276.0
$m_{\tilde{e}_L}$	327.7	328.1	327.5	326.8	323.1
$m_{\tilde{e}_R}$	218.6	217.0	216.6	217.1	228.3
$m_{\tilde{\tau}_1}$	295.9	322.0	370.4	387.7	225.4
$m_{\tilde{\tau}_2}$	372.6	441.2	438.0	549.5	457.0
$m_{\tilde{\nu}_e}$	318.4	318.3	318.1	317.3	313.4
$m_{\tilde{\nu}_\tau}$	354.3	408.0	386.2	499.0	398.4
$m_{\tilde{u}_L}$	1046.1	1045.8	1042.1	1041.8	1041.9
$m_{\tilde{u}_R}$	1003.5	1003.2	1000.0	999.6	997.6
$m_{\tilde{d}_L}$	1049.0	1048.7	1045.1	1044.8	1044.9
$m_{\tilde{d}_R}$	1005.9	1005.6	1001.9	1001.8	1002.3
$m_{\tilde{t}_1}$	948.0	971.1	955.7	971.4	983.5
$m_{\tilde{t}_2}$	1147.0	1155.0	1187.9	1167.6	1175.2
$m_{\tilde{b}_1}$	1022.3	1016.7	1029.9	1021.7	1007.9
$m_{\tilde{b}_2}$	1108.4	1119.6	1137.6	1130.6	1135.5
$m_{\tilde{g}}$	1155.5	1156.5	1154.2	1154.7	1155.0
m_h	115.0	116.4	117.2	117.3	116.8
m_H	762.4	658.5	770.7	637.4	635.9
m_A	761.6	658.5	770.8	637.6	635.9
m_{H^\pm}	766.7	663.9	775.1	642.9	641.0
$\text{BR}(b \rightarrow s\gamma)$	3.70×10^{-4}	4.16×10^{-4}	3.20×10^{-4}	2.89×10^{-4}	2.91×10^{-4}
$\text{BR}(B_s \rightarrow \mu^+\mu^-)$	2.89×10^{-9}	2.10×10^{-9}	3.06×10^{-9}	6.76×10^{-9}	6.68×10^{-9}
Ωh^2	0.110	0.108	0.110	0.108	0.106
$\sigma(\tilde{\chi}p)^{\text{SI}}$ [pb]	2.92×10^{-11}	1.39×10^{-10}	1.01×10^{-10}	2.90×10^{-10}	2.89×10^{-10}

Table 2: Masses (in GeV), B-physics observables, relic density and spin-independent neutralino–proton scattering cross section for points A–E.

References

- [1] H. Georgi and S. L. Glashow, “Unity Of All Elementary Particle Forces,” *Phys. Rev. Lett.* **32** (1974) 438;
H. Georgi, H. R. Quinn and S. Weinberg, “Hierarchy Of Interactions In Unified Gauge Theories,” *Phys. Rev. Lett.* **33** (1974) 451.
- [2] S. Dimopoulos, S. Raby and F. Wilczek, “Supersymmetry And The Scale Of Unification,” *Phys. Rev. D* **24** (1981) 1681.
- [3] D. B. Fairlie, “Higgs’ Fields And The Determination Of The Weinberg Angle,” *Phys. Lett. B* **82** (1979) 97;
N. S. Manton, “A New Six-Dimensional Approach To The Weinberg-Salam Model,” *Nucl. Phys. B* **158** (1979) 141;
Y. Hosotani, “Dynamical Mass Generation By Compact Extra Dimensions,” *Phys. Lett. B* **126** (1983) 309.
- [4] W. Buchmüller, K. Hamaguchi, O. Lebedev and M. Ratz, “Supersymmetric standard model from the heterotic string,” *Phys. Rev. Lett.* **96** (2006) 121602 [arXiv:hep-ph/0511035] and *Nucl. Phys. B* **785** (2007) 149 [arXiv:hep-th/0606187];
O. Lebedev, H. P. Nilles, S. Raby, S. Ramos-Sánchez, M. Ratz, P. K. S. Vaudrevange and A. Wingerter, “A mini-landscape of exact MSSM spectra in heterotic orbifolds,” *Phys. Lett. B* **645** (2007) 88 [arXiv:hep-th/0611095].
- [5] H. P. Nilles, S. Ramos-Sánchez, M. Ratz and P. K. S. Vaudrevange, “From strings to the MSSM,” arXiv:0806.3905 [hep-th].
- [6] Y. Kawamura, “Triplet-doublet splitting, proton stability and extra dimension,” *Prog. Theor. Phys.* **105** (2001) 999 [arXiv:hep-ph/0012125];
G. Altarelli and F. Feruglio, “SU(5) grand unification in extra dimensions and proton decay,” *Phys. Lett. B* **511** (2001) 257 [arXiv:hep-ph/0102301];
L. J. Hall and Y. Nomura, “Gauge unification in higher dimensions,” *Phys. Rev. D* **64** (2001) 055003 [arXiv:hep-ph/0103125];
A. Hebecker and J. March-Russell, “A minimal S(1)/(Z(2) x Z'(2)) orbifold GUT,” *Nucl. Phys. B* **613** (2001) 3 [arXiv:hep-ph/0106166];
T. Asaka, W. Buchmüller and L. Covi, “Gauge unification in six dimensions,” *Phys. Lett. B* **523** (2001) 199 [arXiv:hep-ph/0108021];
L. J. Hall, Y. Nomura, T. Okui and D. Tucker-Smith, “SO(10) unified theories in six dimensions,” *Phys. Rev. D* **65** (2002) 035008 [arXiv:hep-ph/0108071].
- [7] V. S. Kaplunovsky, “Mass Scales Of The String Unification,” *Phys. Rev. Lett.* **55**, 1036 (1985).
- [8] L. E. Ibáñez and D. Lüst, “Duality anomaly cancellation, minimal string unification and the effective low-energy Lagrangian of 4-D strings,” *Nucl. Phys. B* **382** (1992) 305 [arXiv:hep-th/9202046].
- [9] E. Witten, “Strong Coupling Expansion Of Calabi-Yau Compactification,” *Nucl. Phys. B* **471** (1996) 135 [arXiv:hep-th/9602070].

- [10] A. Hebecker and M. Trapletti, “Gauge unification in highly anisotropic string compactifications,” Nucl. Phys. B **713** (2005) 173 [arXiv:hep-th/0411131].
- [11] B. Dundee, S. Raby and A. Wingerter, “Reconciling Grand Unification with Strings by Anisotropic Compactifications,” arXiv:0805.4186 [hep-th];
B. Dundee and S. Raby, “On the string coupling in a class of stringy orbifold GUTs,” arXiv:0808.0992 [hep-th].
- [12] G. Burdman and Y. Nomura, “Unification of Higgs and gauge fields in five dimensions,” Nucl. Phys. B **656** (2003) 3 [arXiv:hep-ph/0210257].
- [13] Y. Nomura, D. Poland and B. Tweedie, “Holographic Grand Unification,” JHEP **0612** (2006) 002 [arXiv:hep-ph/0605014].
- [14] H. M. Lee, H. P. Nilles and M. Zucker, “Spontaneous localization of bulk fields: The six-dimensional case,” Nucl. Phys. B **680** (2004) 177 [arXiv:hep-th/0309195].
- [15] W. Buchmüller, C. Lüdeling and J. Schmidt, “Local SU(5) Unification from the Heterotic String,” JHEP **0709** (2007) 113 [arXiv:0707.1651 [hep-ph]];
W. Buchmüller, R. Catena and K. Schmidt-Hoberg, “Small Extra Dimensions from the Interplay of Gauge and Supersymmetry Breaking,” Nucl. Phys. B **804** (2008) 70 [arXiv:0803.4501 [hep-ph]].
- [16] P. Hosteins, R. Kappl, M. Ratz and K. Schmidt-Hoberg, “Gauge-top unification,” arXiv:0905.3323 [hep-ph].
- [17] N. Haba and Y. Shimizu, “Gauge-Higgs unification in the 5 dimensional E(6), E(7), and E(8) GUTs on orbifold,” Phys. Rev. D **67** (2003) 095001 [Erratum-ibid. D **69** (2004) 059902] [arXiv:hep-ph/0212166];
I. Gogoladze, Y. Mimura and S. Nandi, “Gauge Higgs unification on the left-right model,” Phys. Lett. B **560** (2003) 204 [arXiv:hep-ph/0301014];
I. Gogoladze, Y. Mimura and S. Nandi, “Unification of gauge, Higgs and matter in extra dimensions,” Phys. Lett. B **562** (2003) 307 [arXiv:hep-ph/0302176];
A. Hebecker and M. Ratz, “Group-theoretical aspects of orbifold and conifold GUTs,” Nucl. Phys. B **670** (2003) 3 [arXiv:hep-ph/0306049];
I. Gogoladze, T. Li, V. N. Senoguz and Q. Shafi, “Non-canonical MSSM, unification, and new particles at the LHC,” Phys. Rev. D **74** (2006) 126006 [arXiv:hep-ph/0608181];
Y. Mimura and S. Nandi, “Three family unification in higher dimensional models,” arXiv:0902.4275 [hep-ph];
Y. Mimura, “Flavor Symmetry in Gauge-Higgs-Matter Unified Orbifold GUTs,” arXiv:0903.1875 [hep-ph].
- [18] K. w. Choi, N. y. Haba, K. S. Jeong, K. i. Okumura, Y. Shimizu and M. Yamaguchi, “Electroweak symmetry breaking in supersymmetric gauge-Higgs unification models,” JHEP **0402** (2004) 037 [arXiv:hep-ph/0312178].
- [19] G. Lopes Cardoso, D. Lüst and T. Mohaupt, “Moduli spaces and target space duality symmetries in (0,2) Z(N) orbifold theories with continuous Wilson lines,” Nucl. Phys. B **432** (1994) 68 [arXiv:hep-th/9405002].

- [20] I. Antoniadis, E. Gava, K. S. Narain and T. R. Taylor, “Effective μ term in superstring theory,” Nucl. Phys. B **432** (1994) 187 [arXiv:hep-th/9405024].
- [21] A. Brignole, L. E. Ibáñez, C. Muñoz and C. Scheich, “Some Issues In Soft Susy Breaking Terms From Dilaton / Moduli Sectors,” Z. Phys. C **74** (1997) 157 [arXiv:hep-ph/9508258];
 A. Brignole, L. E. Ibáñez and C. Muñoz, “Orbifold-induced μ term and electroweak symmetry breaking,” Phys. Lett. B **387** (1996) 769 [arXiv:hep-ph/9607405];
 A. Brignole, L. E. Ibáñez and C. Muñoz, “Soft supersymmetry-breaking terms from supergravity and superstring models,” arXiv:hep-ph/9707209.
- [22] T. Kobayashi and K. Yoshioka, “Kaluza-Klein mediated supersymmetry breaking,” Phys. Rev. Lett. **85** (2000) 5527 [arXiv:hep-ph/0008069];
 Z. Chacko and M. A. Luty, “Radion mediated supersymmetry breaking,” JHEP **0105** (2001) 067 [arXiv:hep-ph/0008103].
- [23] G. F. Giudice and A. Masiero, “A Natural Solution to the μ Problem in Supergravity Theories,” Phys. Lett. B **206** (1988) 480.
- [24] V. S. Kaplunovsky and J. Louis, “Model independent analysis of soft terms in effective supergravity and in string theory,” Phys. Lett. B **306** (1993) 269 [arXiv:hep-th/9303040].
- [25] A. Hebecker, J. March-Russell and R. Ziegler, “Inducing the μ and the $B\mu$ Term by the Radion and the 5d Chern-Simons Term,” arXiv:0801.4101 [hep-ph].
- [26] N. Arkani-Hamed, A. G. Cohen and H. Georgi, “Anomalies on orbifolds,” Phys. Lett. B **516** (2001) 395 [arXiv:hep-th/0103135];
 C. A. Scrucca, M. Serone, L. Silvestrini and F. Zwirner, “Anomalies in orbifold field theories,” Phys. Lett. B **525** (2002) 169 [arXiv:hep-th/0110073];
 R. Barbieri, R. Contino, P. Creminelli, R. Rattazzi and C. A. Scrucca, “Anomalies, Fayet-Iliopoulos terms and the consistency of orbifold field theories,” Phys. Rev. D **66** (2002) 024025 [arXiv:hep-th/0203039].
- [27] C. A. Scrucca and M. Serone, “Anomalies in field theories with extra dimensions,” Int. J. Mod. Phys. A **19**, 2579 (2004) [arXiv:hep-th/0403163].
- [28] A. Djouadi, J. L. Kneur and G. Moultaka, “SuSpect: A Fortran code for the supersymmetric and Higgs particle spectrum in the MSSM,” Comput. Phys. Commun. **176** (2007) 426 [arXiv:hep-ph/0211331],
<http://www.lpta.univ-montp2.fr/users/kneur/Suspect/>
- [29] D. Martí and A. Pomarol, “Supersymmetric theories with compact extra dimensions in $N = 1$ superfields,” Phys. Rev. D **64** (2001) 105025 [arXiv:hep-th/0106256].
- [30] N. Arkani-Hamed, T. Gregoire and J. G. Wacker, “Higher dimensional supersymmetry in 4D superspace,” JHEP **0203** (2002) 055 [arXiv:hep-th/0101233].
- [31] A. Hebecker, “5D super Yang-Mills theory in 4-D superspace, superfield brane operators, and applications to orbifold GUTs,” Nucl. Phys. B **632** (2002) 101 [arXiv:hep-ph/0112230].

- [32] N. Seiberg, “Five dimensional SUSY field theories, non-trivial fixed points and string dynamics,” *Phys. Lett. B* **388** (1996) 753 [arXiv:hep-th/9608111];
K. A. Intriligator, D. R. Morrison and N. Seiberg, “Five-dimensional supersymmetric gauge theories and degenerations of Calabi-Yau spaces,” *Nucl. Phys. B* **497** (1997) 56 [arXiv:hep-th/9702198].
- [33] A. Hebecker and A. Westphal, “Gauge unification in extra dimensions: Power corrections vs. higher-dimension operators,” *Nucl. Phys. B* **701** (2004) 273 [arXiv:hep-th/0407014].
- [34] R. Barbieri and A. Strumia, “The ‘LEP paradox’,” arXiv:hep-ph/0007265;
J. A. Casas, J. R. Espinosa and I. Hidalgo, “The MSSM fine tuning problem: A Way out,” *JHEP* **0401** (2004) 008 [arXiv:hep-ph/0310137];
R. Kitano and Y. Nomura, “A solution to the supersymmetric fine-tuning problem within the MSSM,” *Phys. Lett. B* **631** (2005) 58 [arXiv:hep-ph/0509039];
G. F. Giudice and R. Rattazzi, “Living dangerously with low-energy supersymmetry,” *Nucl. Phys. B* **757** (2006) 19 [arXiv:hep-ph/0606105].
- [35] C. Amsler *et al.* [Particle Data Group], “Review of particle physics,” *Phys. Lett. B* **667** (2008) 1.
- [36] LEP2 SUSY Working Group [ALEPH, DELPHI, L3 and OPAL experiments],
<http://lepsusy.web.cern.ch/lepsusy/>
- [37] S. Schael *et al.* [ALEPH, DELPHI, L3 and OPAL Collaborations, and the LEP Working Group on Higgs Boson Searches], “Search for neutral MSSM Higgs bosons at LEP,” *Eur. Phys. J. C* **47** (2006) 547 [arXiv:hep-ex/0602042].
- [38] G. Degrossi, S. Heinemeyer, W. Hollik, P. Slavich and G. Weiglein, “Towards high-precision predictions for the MSSM Higgs sector,” *Eur. Phys. J. C* **28** (2003) 133 [arXiv:hep-ph/0212020].
- [39] E. Barberio *et al.* [Heavy Flavor Averaging Group], “Averages of b -hadron and c -hadron Properties at the End of 2007,” arXiv:0808.1297 [hep-ex].
- [40] M. Misiak *et al.*, “Estimate of $\text{BR}(B \rightarrow X_s \gamma)$ at $\mathcal{O}(\alpha_s^2)$ ” *Phys. Rev. Lett.* **98** (2007) 022002 [arXiv:hep-ph/0609232].
- [41] T. Aaltonen *et al.* [CDF Collaboration], “Search for $B_s \rightarrow \mu^+ \mu^-$ and $B_d \rightarrow \mu^+ \mu^-$ Decays with 2fb^{-1} of $p\bar{p}$ Collisions,” *Phys. Rev. Lett.* **100** (2008) 101802 [arXiv:0712.1708 [hep-ex]].
- [42] J. Dunkley *et al.* [WMAP Collaboration], “Five-Year Wilkinson Microwave Anisotropy Probe (WMAP) Observations: Likelihoods and Parameters from the WMAP data,” arXiv:0803.0586 [astro-ph].
- [43] G. Belanger, F. Boudjema, A. Pukhov and A. Semenov, “micrOMEGAs2.0: A program to calculate the relic density of dark matter in a generic model,” *Comput. Phys. Commun.* **176** (2007) 367 [arXiv:hep-ph/0607059]; arXiv:0803.2360 [hep-ph].

- [44] H. Baer, C. h. Chen, F. Paige and X. Tata, “Signals for minimal supergravity at the CERN large hadron collider: Multi - jet plus missing energy channel,” *Phys. Rev. D* **52** (1995) 2746 [arXiv:hep-ph/9503271].
- [45] H. Baer, C. h. Chen, F. Paige and X. Tata, “Signals for Minimal Supergravity at the CERN Large Hadron Collider II: Multilepton Channels,” *Phys. Rev. D* **53** (1996) 6241 [arXiv:hep-ph/9512383].
- [46] A. Hebecker, J. March-Russell and T. Yanagida, “Higher-dimensional origin of heavy sneutrino domination and low-scale leptogenesis,” *Phys. Lett. B* **552** (2003) 229 [arXiv:hep-ph/0208249].
- [47] F. Borzumati and A. Masiero, “Large Muon And Electron Number Violations In Supergravity Theories,” *Phys. Rev. Lett.* **57** (1986) 961.
- [48] S. P. Martin and M. T. Vaughn, “Two Loop Renormalization Group Equations For Soft Supersymmetry Breaking Couplings,” *Phys. Rev. D* **50** (1994) 2282 [Erratum-*ibid.* *D* **78** (2008) 039903] [arXiv:hep-ph/9311340].
- [49] J. L. Evans, D. E. Morrissey and J. D. Wells, “Higgs boson exempt no-scale supersymmetry and its collider and cosmology implications,” *Phys. Rev. D* **75** (2007) 055017 [arXiv:hep-ph/0611185].
- [50] G. A. Blair, W. Porod and P. M. Zerwas, “Reconstructing supersymmetric theories at high energy scales,” *Phys. Rev. D* **63** (2001) 017703 [arXiv:hep-ph/0007107] and “The reconstruction of supersymmetric theories at high energy scales.” *Eur. Phys. J. C* **27** (2003) 263 [arXiv:hep-ph/0210058].